Sensors & Actuators: A. Physical 355 (2023) 114331

Contents lists available at ScienceDirect

Sensors and Actuators: A. Physical

journal homepage: www.journals.elsevier.com/sensors-and-actuators-a-physical

Advances in triboelectric pressure sensors

Linan Guo, Guitao Wu *, Qunyi Wang, Tong Li, Bohan Yao, Yongjiu Zou *, Minyi Xu *

Dalian Key Lab of Marine Micro/Nano Energy and Self-powered System, Marine Engineering College, Dalian Maritime University, Dalian 116026, China

ARTICLE INFO

Keywords:
Triboelectric nanogenerators
Pressure sensors
Electrode material
Internet of Things

ABSTRACT

Pressure sensors are widely used in various industrial automatic-control environments. With the rapid development of the Internet of Things (IoT) technology, the requirements for environmental adaptability and reliability of pressure sensors in IoT applications are also increasing; moreover, pressure sensors are challenged by the energy supply problem. In this regard, a triboelectric pressure sensor has the remarkable characteristic of being self-powered. It is highly sensitive, stable, and environmentally adaptable, all of whose features are of considerable significance for fully adapting to the development needs of IoT. The environmental adaptability and performance stability of triboelectric pressure sensors in information sensing systems are gradually increasing, which also puts forward higher requirements for material selection and processing technology. In this study, the basic working principle, structural design, electrode material, processing technology, sensing characteristics, and various application scenarios of triboelectric pressure sensors are systematically and comprehensively summarised. Furthermore, following a novel approach, triboelectric pressure sensors are divided into four types according to the electrode materials: conductor, semiconductor, hybrid, and hydrogel electrodes. Finally, the existing challenges and future application prospects are discussed in depth. The study findings can contribute to promoting further developments in the field.

1. Introduction

The rapid development of the Internet of Things (IoT) in recent years has made the realisation of the Internet of Everything (IoE) through mobile networks and intelligent terminal devices gradually feasible [1–6]. The vision of the IoE is reflected in the wide application of the IoT in electronic skin (e-skin)[7–14], sports health monitoring [15–22], human–computer interaction systems [23–30], and other fields. However, a sizable number of sensor systems are required to realise the IoE. A significant amount of tactile and pressure sensing [31–36] information must be conveyed through pressure sensors as a medium when creating a connection between the mobile Internet and the physical terminal information interaction. Sensors need to be stretchable, flexible, and biocompatible in e-skin applications. In sports health-monitoring applications, pressure sensors must have the capacity to be miniaturised, lightweight and intelligent. Sensitivity and stability are required in human–computer interaction applications. Owing to these myriad requirements, research has recently focused on pressure sensors with improved adaptability [37–40], higher performance [41–45], and more precise manufacturing processes [46–51].

Piezoresistive, capacitive, piezoelectric, and other types of pressure sensors have become widely used in recent years. Piezoresistive sensors [52–56] refer to sensors based on the piezoresistive effect of a single-crystal silicon material. The resistivity of monocrystalline silicon materials varies with the applied force, and the measurement circuit can produce an electrical signal output that is proportional to the applied force. Capacitive sensors [57–61] generally use a round metal film or metal-plated film as the electrode of the capacitor. When the film perceives pressure and deforms, the capacitance formed between the film and the fixed electrode changes, and the measuring circuit can output an electrical signal that has a certain relationship with the voltage. These two types of sensors require an external power supply while working, which considerably limits the applicability of piezoresistive and capacitive sensors in harsh working environments. Piezoelectric pressure sensors [62–69] convert the measured pressure into electrical signals via the piezoelectric effect. The quantity of charge produced by piezoelectric elements constructed from piezoelectric materials under pressure and the applied force has a linear relationship. Although piezoelectric pressure sensors successfully resolve the problem of external power supply, they can only be used in common application environments, owing to the limitations of there being only a few types of piezoelectric materials [70–74]. Therefore, it is necessary to develop a new type of

* Corresponding authors.
E-mail addresses: wuguitao@dlmu.edu.cn (G. Wu), zouyj0421@dlmu.edu.cn (Y. Zou), xuminyi@dlmu.edu.cn (M. Xu).

https://doi.org/10.1016/j.sna.2023.114331
Received 8 February 2023; Received in revised form 10 March 2023; Accepted 24 March 2023
Available online 26 March 2023

pressure sensor with strong applicability, high sensitivity, and self-power supply [75–82], which can revolutionize the field of pressure sensors.

In 2012, Professor Wang Zhonglin first proposed a triboelectric nanogenerator (TENG). The materials and structures of TENGs have been continuously optimised owing to several years of development, thereby endowing them with the advantages of large output, high efficiency, and good stability [83–92]. In addition, flexible TENGs can adjust to different deformations during usage, including stretching, twisting, and bending [93–99]. Hence, self-powered pressure sensors based on the concept of triboelectric generators have been fabricated and used frequently in recent years[100–104]. Many structural optimisations and experimental investigations have been carried out to improve the working applicability and sensitivity of pressure sensors and to broaden the range of detection [105–109]. In terms of material selection, in addition to research on the modification of triboelectric materials, studies have also been conducted on electrode materials. This study focussed on different types of electrode materials, as illustrated in Fig. 1, and introduced recent advances in the selection of electrode materials for triboelectric pressure sensors. Common electrode materials include copper[110–118], silver [119–124], carbon [125–136], polymer hybrid electrode materials [137–140], and flexible ion-gel electrode materials [141–146]. In terms of changing the physical structure, different contact mechanisms have been designed by constructing surface micro–nanostructures [147–150]. In processing technology, various physical [151–155] and chemical [156–158] properties of the surface treatment process have been applied.

In this study, we provide a comprehensive overview of triboelectric pressure sensors with different types of electrode materials. First, triboelectric pressure sensors were divided into four types based on the different electrode materials. Then, the features of each type of triboelectric pressure sensor were analysed in detail, including the structural design, working principle, sensing performance analysis, and application scenario discussion. Finally, we discuss the problems and future developmental trends in triboelectric pressure sensors. This study will serve as a reference for selecting and processing electrode materials for triboelectric pressure sensors, which will help develop intelligent sensing systems in the future.

2. Fundamental mechanism of triboelectric pressure sensors

2.1. Theory of triboelectric nanogenerators

To explain the working principle of TENGs, theoretical investigations such as analysing the Maxwell displacement current by combining the characteristics of various power generation effects, such as piezoelectric and triboelectric effects, have been performed. Wang's group derived the expanded Maxwell's equations for a mechano-driven slow-moving media system recently [159–162].

$$\nabla \cdot \boldsymbol{D}' = \rho_f - \nabla \cdot P_s \tag{1}$$

$$\nabla \cdot \boldsymbol{B} = 0 \tag{2}$$

$$\nabla \times (\boldsymbol{E} - \boldsymbol{v} \times \boldsymbol{B}) = -\frac{\partial \boldsymbol{B}}{\partial t} \tag{3}$$

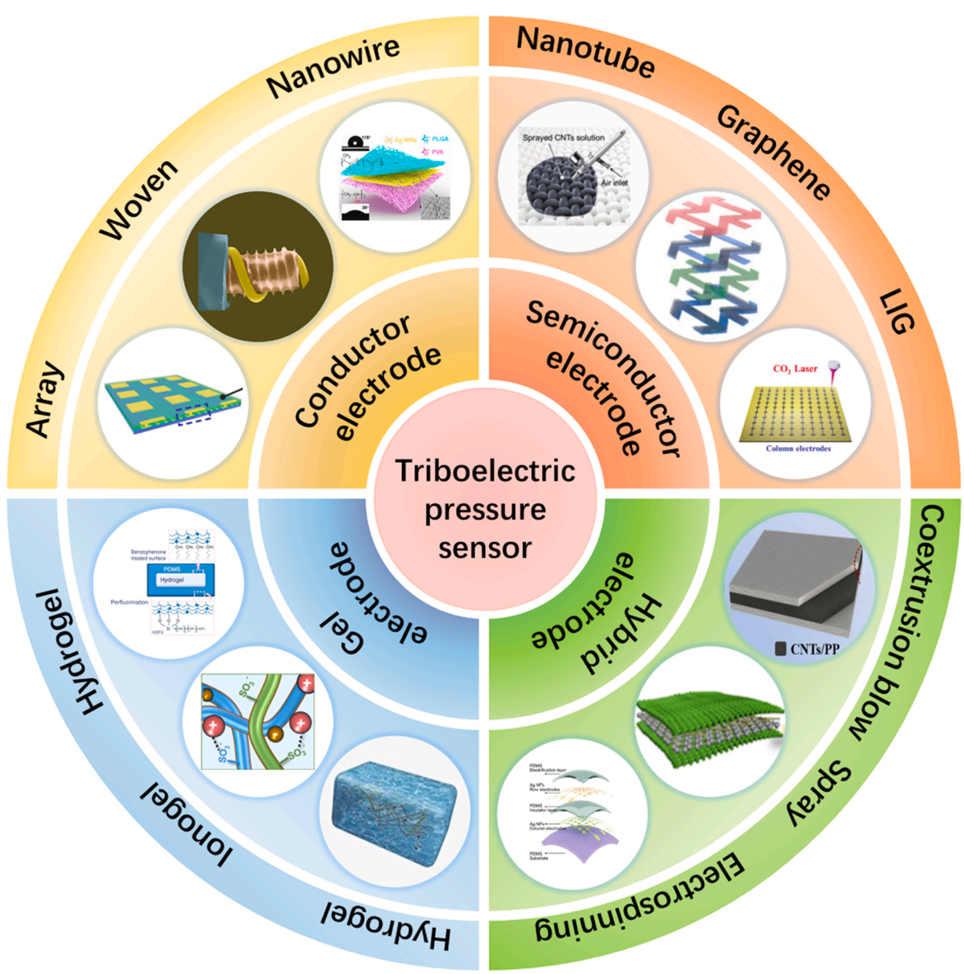

Fig. 1. Classification of triboelectric pressure sensors based on the electrode materials.

$$\nabla \times [\boldsymbol{H} + \boldsymbol{v} \times (\boldsymbol{D}' + P_s)] = \boldsymbol{J}_f + \rho_f v + \frac{\partial P_s}{\partial t} + \frac{\partial \boldsymbol{D}'}{\partial t} \tag{4}$$

where $\boldsymbol{D}'$ is the electric displacement field, ρ_f is the space charge density of free charges, P_s is a polarization term in the displacement vector, $\boldsymbol{B}$ is the magnetic field, $\boldsymbol{E}$ is electromagnetic field, v is the translation velocity, $\boldsymbol{H}$ is the magnetizing field, $\boldsymbol{J}_f$ is the local free electric current density, which primarily expand the applications of TENG in various fields.

In the case of TENGs, triboelectric charges are produced on surfaces simply due to a physical contact between two different materials. To account for the contribution made by the contact electrification induced electrostatic charges in the Maxwell's equations, an additional term P_s is added in $\boldsymbol{D}'$. P_s is mainly due to the existence of the surface charges that are independent of the presence of electric field.

2.2. Theory of triboelectric pressure sensors

There are four working modes for a TENG: vertical contact–separation, lateral sliding, single-electrode, and freestanding triboelectric-layer modes. Triboelectric pressure sensors mainly operate in the vertical contact–separation mode, which is one of the four working principles that constitute the TENG's primary operating modes. This mode places two materials, which have distinct triboelectric characteristics, opposite to each other vertically. Two triboelectric layers come into contact with each other when subjected to external excitation. The surfaces of the two triboelectric layers generate electric charges with opposing characteristics owing to electrostatic induction, as shown in Fig. 2a. When the external excitation is withdrawn, the two triboelectric layers split, creating a potential drop between the two electrodes. As shown in Fig. 2b, this causes electrons to flow through the linked load. When the outer triboelectric layer is released to the limit position, the voltage between the two electrodes reaches the maximum. Fig. 2c shows the physical model of the triboelectric layers and the electrode layers in this state. The triboelectric layers close when an external excitation is applied again. As shown in Fig. 2d, electrons transfer during pressing and the voltage between the electrodes disappears gradually. This further enables electrons to return to achieve electrical equilibrium. This mode requires efficient cycle switching between the intimate contact state and the completely separated state for the proper functioning of the friction power-production process [100].

According to the equivalent physical model illustrated in Fig. 2c, the electric field strength, obtained from the Gauss theorem, in each region is given by.

Inside the air gap

$$E_0 = \frac{\sigma_0 - \frac{Q}{S}}{\varepsilon_0} \tag{5}$$

Inside the dielectric layer 1

$$E_1 = \frac{-Q}{\varepsilon_0 \varepsilon_1 S}. \tag{6}$$

Inside the dielectric layer 2

$$E_2 = \frac{-Q}{\varepsilon_0 \varepsilon_2 S}. \tag{7}$$

Here, σ_0 is the triboelectric charge density; ε_0 is the permittivity in a vacuum; Q is the amount of transferred charge; and ε_1 is the relative dielectric constant of the dielectric layer.

The voltage between the two electrodes can be given by

$$V = E \cdot d_{(t)} + E_1 \cdot d_1 + E_2 \cdot d_2. \tag{8}$$

Substituting Eqs. (5), (6) and (7) in Eq. (8) implies

$$V = -\frac{Q}{\varepsilon_0 \cdot S}\left(\frac{d_1}{\varepsilon_1} + d_{(t)} + \frac{d_2}{\varepsilon_2}\right) + \frac{\sigma_0 d_{(t)}}{\varepsilon_0} \tag{9}$$

where d_1, d_2, and $d_{(t)}$ represent the thickness of dielectric layer 1, dielectric layer 2, and the air gap distance, respectively. In the open-circuit condition, there is no charge transfer, which means that Q is zero. In this case, the open-circuit voltage V_{OC} is given by

$$V_{OC} = \frac{\sigma_0 d_{(t)}}{\varepsilon_0}. \tag{10}$$

According to Eq. (10), in theory, the dielectric constant of the material is a constant value in determining the TENG pressure sensor of the material. Therefore, the microstructure of the dielectric layer can be regarded as a gap layer, and theoretically, the change in voltage has a linear relationship with the change in the gap. This has been confirmed

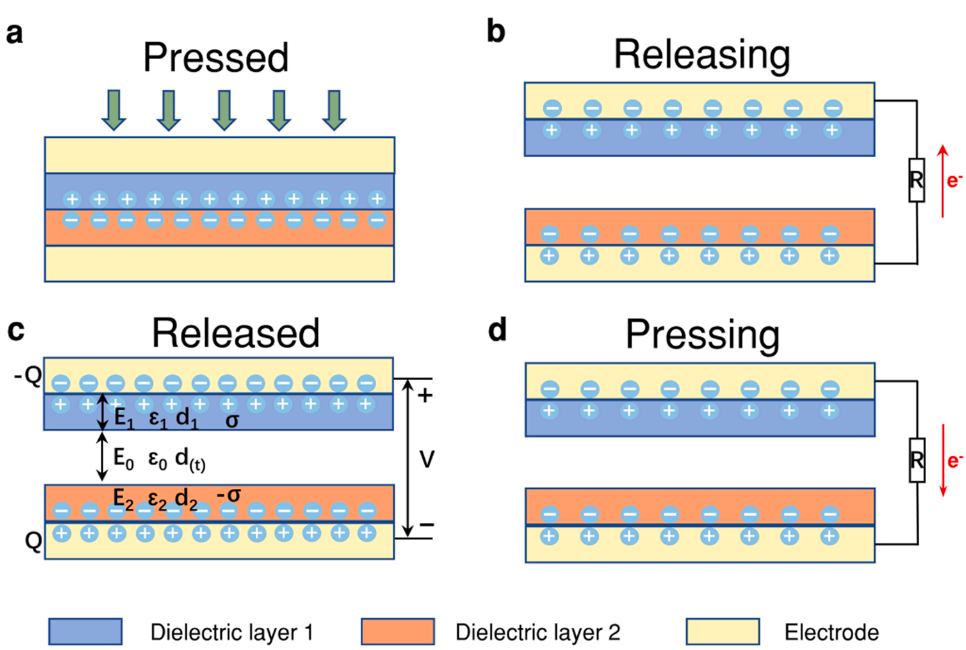

Fig. 2. Working mechanism of the vertical contact–separation mode of TENG. (a) Contact electrification under pressure. (b) Electrons transfer during releasing. (c) Equivalent physical model. (d) Electrons transfer during pressing.

by previous research [163–165].

3. Triboelectric pressure sensor

Most materials in nature have different electronegativities. Various materials can be used as triboelectric layers of TENG. Different contact materials couple to produce different triboelectric effects. Material selection for the TENG contact layer, material processing technology, and other elements have been extensively studied. And the studies have reported positive experimental findings, proving TENG appropriate for various scenarios and showing a stronger triboelectric effect. Self-powered sensors using a variety of electrode materials exhibit outstanding sensing capabilities when used in various scenarios. For instance, sensors have been fabricated from ion-gel electrode materials, metal electrode materials, semiconductor electrode materials, and hybrid electrode materials made of metal, semiconductor, and polymer materials. Consequently, there are numerous triboelectric material varieties to choose from when making material decisions.

3.1. Triboelectric pressure sensor based on metal conductor electrodes

Metal conductor electrode materials are the most widely used electrode materials in current research. Common metal conductor materials are characterised by low cost, excellent conductivity, and good mechanical strength. In addition, individual materials have unique characteristics. For example, aluminum and copper have good stability and durability, making them suitable TENG electrode materials in humid environments. Silver and gold have excellent ductility, which can be used in e-skin applications. The application of silver nanowires (AgNWs) is the most representative processing technology, which fully demonstrates their excellent ductility.

3.1.1. Two-dimensional planar structure

A two-dimensional planar-structure electrode is the most common structure of the electrode materials used in triboelectric pressure sensors. Wang et al. [47] developed a discrete, self-powered, integrated triboelectric sensor array (ITSA). The main structural features of a single-sensor unit are shown in Fig. 3a. Silicone substrates were used for the top and bottom layers. The top and bottom electrode layers were made of metal-deposited fabrics, which not only maintain the excellent conductivity of the metal but also make the electrode layer highly flexible with the use of metal deposition technology. The electrode contacts the triboelectric layer significantly under different pressure excitations, such that the sensing performance of the device remains stable. Fig. 3b shows the voltage feedback of each sensor unit in the structure of the ITSA under an 'N' type external pressure excitation. It can be seen in the figure that there are obvious voltage signal differences between the pressurised and non-pressurised units. The shape of the

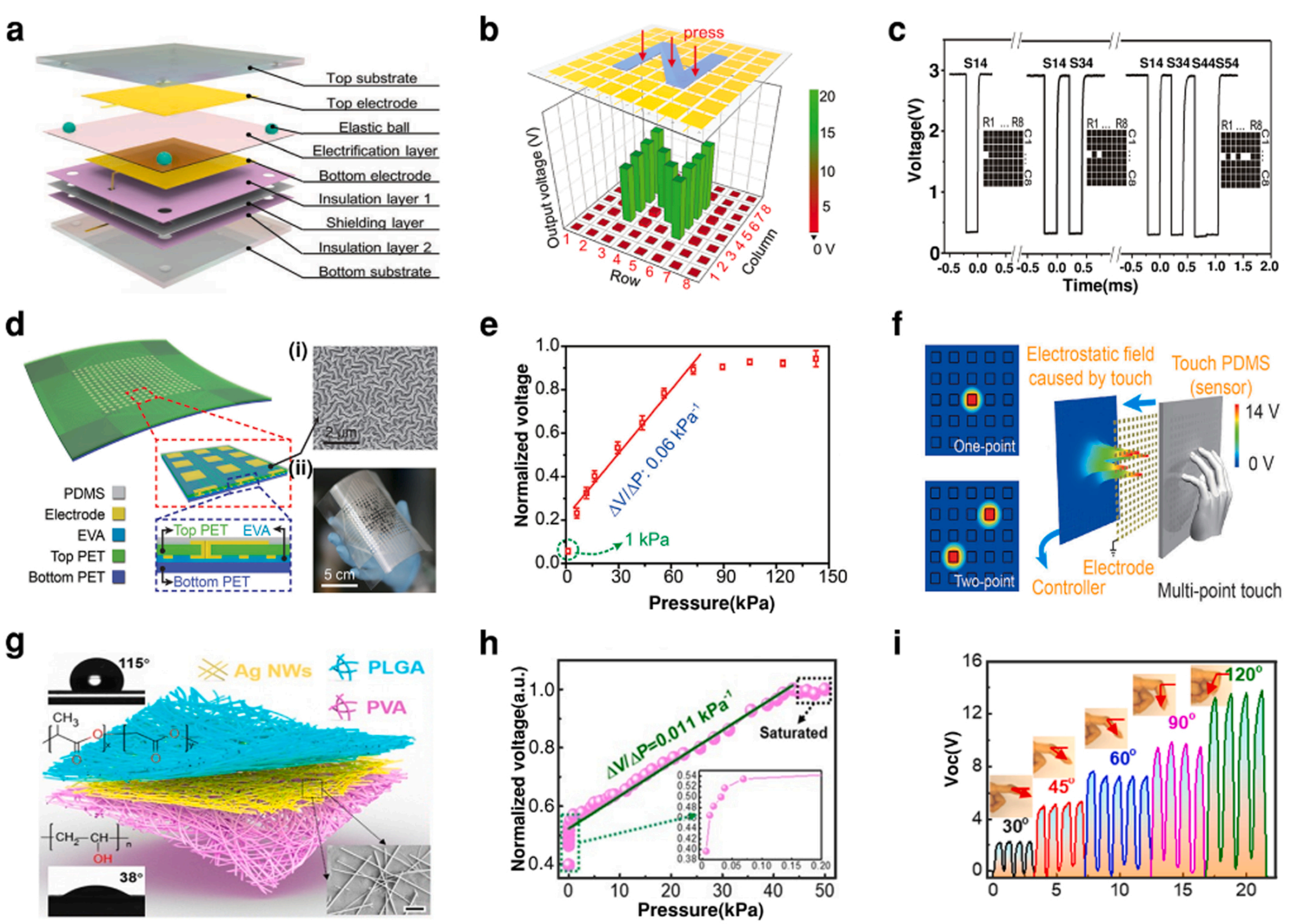

Fig. 3. Two-dimensional planar structure electrode. (a) Structure of a single sensor unit of a triboelectric sensor array (TSA). (b) Output voltage curves of the TSA when a model of shape 'N' is pressed on the top surface. (c) Tests with different numbers of points. (d) Structure of the triboelectric sensor matrices (TESMs). (e) Output voltage as a function of pressure. (f) Schematic of the pressure mapping process. (g) Structural design of the all-nanofiber triboelectric e-skin. (h) Normalized output voltage response to a wide range of pressure. (i) Detection of the finger bending angles by attaching an e-skin to the knuckle.
(a-c) Reproduced with permission [47] (Copyright 2020, Wiley-VCH). (d-f) Reproduced with permission [84] (Copyright 2016, Wiley-VCH). (g-i) Reproduced with permission [95] (Copyright 2020, Amer Assoc Advancement Science).

mapped 'N′ can also be observed. The ITSA was combined with a microprogrammed control unit (MCU-MSP430) to realise the visualisation functions of pressure monitoring and position recognition. Fig. 3c shows that the visualisation function exhibits excellent performance in multi-point simultaneous monitoring. These results verify the practicability of the ITSA in pressure mapping and position recognition. Furthermore, the integration of the ITSA and wireless sensor system can realise the remote monitoring function of the contact objects.

To improve the manufacturing accuracy of the electrode arrays, Wang et al. [84] applied a deposition process to fabricate patterned electrode arrays. They proposed flexible triboelectric sensor matrices (TESMs) that realise real-time tactile pressure sensing. The main structure is shown in Fig. 3d. The top flexible substrate of a single sensing unit was made of a polyethylene glycol terephthalate (PET) film. The bottom electrode was enclosed in a layer of PET film and ethylene-vinyl acetate (EVA) copolymer. The top electrified triboelectric layer was composed of a layer of polydimethylsiloxane (PDMS) spin coating. Fig. 3d-(i) shows the surface microstructure of PDMS. The TESM electrode was fabricated by the magnetic sputtering process. First, both sides of the top PET film were covered with predesigned masks with different patterns, and then the array through-hole was created by laser cutting. An Ag layer was then deposited on both sides of the substrate using a magnetic sputtering process. The two deposition layers were connected through a laser-cut through-hole. Fig. 3d-(ii) shows the device used in this study. Fig. 3e shows the experimental results of the pressure sensitivity of the device. In the pressure range below 80 kPa, the change rate of $\Delta V/\Delta P$ presents a linear feature, and the pressure sensitivity was 0.06 kPa^{-1}, which is a good pressure sensitivity value. Fig. 3f shows the results of the FEM simulation of single-point and multi-point touch perceptions using Comsol. The difference in the potential distribution between the contact point and non-contact electricity can be observed intuitively. It provides a theoretical basis for the feasibility of TEMS. In the following research, TEMS was integrated with a data processing unit, and with the help of the signal filter program, an excellent path-awareness recognition function was realised. Furthermore, Lee, Zhang, and Wang et al. [166–168] used array-structured metal conductor electrodes to fabricate triboelectric pressure sensor arrays, which exhibited excellent sensitivity and linearity in the low-pressure range (<10 kPa).

By restructuring the material with a microstructure, Xiao et al.[95] designed a flexible and stretchable e-skin based on a TENG, and its structure is shown in Fig. 3g. It is a sandwich structure composed of poly-(lactic co-glycolic acid) (PLGA), AgNWs, and polyvinyl alcohol (PVA). PLGA was used as the triboelectric layer, AgNWs as the flexible electrode layer, and hydrophilic PVA fabric as the skin contact layer. AgNWs have excellent ductility, electrical conductivity, and a high specific surface area, which can be used to prepare electrodes for flexible sensors with high performance and sensitivity. AgNWs have been used in many applications in the development of flexible sensors. Fig. 3h shows the research results for the pressure sensitivity of the e-skin. In the pressure range below 40 kPa, the change rate of $\Delta V/\Delta P$ exhibited a linear relationship, and the pressure sensitivity was 0.011kPa^{-1}. In the experimental research on e-skin for monitoring human movement behaviour, the bending test of fingers (as shown in Fig. 3i) and limbs, and pulse test of the wrist and carotid artery were carried out; the e-skin showed excellent working stability. Bu and Gao et al.[169,170] also used AgNWs as electrode materials to make triboelectric pressure sensors, which had excellent sensitivity of 0.1 nA/kPa and 2.6 mV/Pa in a low-pressure range.

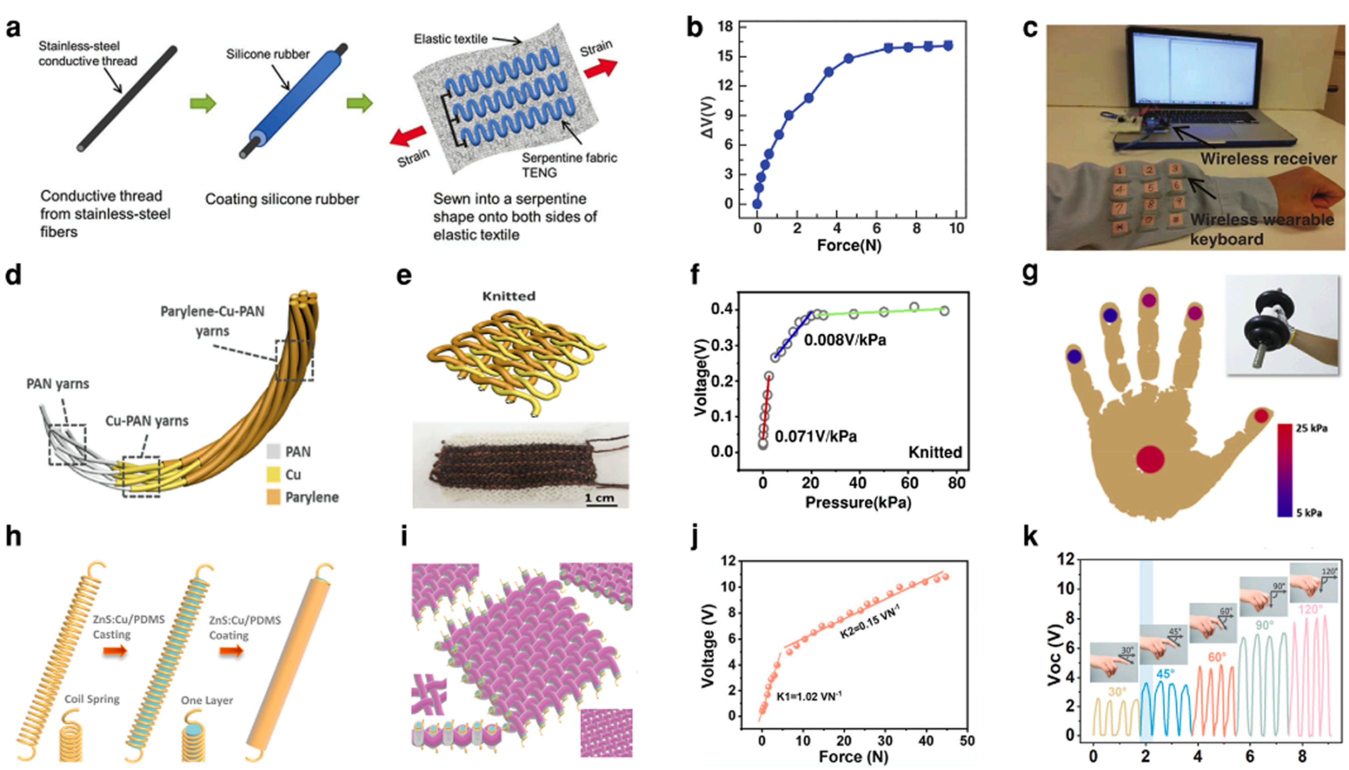

Fig. 4. Woven fabric structure electrode. (a) Structure of a single-wire triboelectric nanogenerator (TENG). (b) Relationship between voltage difference and applied force. (c) Demonstration of triboelectric threads as a wireless wearable keyboard. (d) Schematics of Cu-PAN yarns and parylene-CuPAN yarns. (e) Schematics (top) and photographs (bottom) of textile pressure sensors fabricated by knitting. (f) Pressure response from textile pressure sensors with knitted structures. (g) Voltage signals recorded by different sensors and the corresponding pressure mappings when holding a dumbbell. (h) Schematic showing the preparation process of a TENG. (i) Schematic of the arrays sensing fabric. (j) V_{OC} of TENG as a bending sensor when a finger bends at different angles.(k) The V_{OC} of TENG as a bending sensor when fingers bend at different angles.

(a-c) Reproduced with permission [171] (Copyright 2017, Wiley-VCH). (d-g) Reproduced with permission [172] (Copyright 2020, Elsevier). (h-k) Reproduced with permission [173] (Copyright 2021, Elsevier).

3.1.2. Woven fabric structure

In addition to metal deposition processes and nanotechnology, metal wire coating, winding, and weaving processes are used to prepare flexible electrodes. Lai et al.[171] proposed a single-wire TENG, as shown in Fig. 4a. It works on the principle of a single-electrode TENG, where the electrode material is composed of multiple bundles of stainless steel wires and a soft silica gel material is used as the triboelectric material. These materials can be woven into fabric-type TENGs for static and dynamic force sensing because of their high flexibility. Fig. 4b shows the voltage changes generated by the sensors under various external pressure stimuli. When the applied external force reached 6 N, the voltage change rate of the sensor gradually stabilised. The sensor exhibited excellent linear variation characteristics. Fig. 4c demonstrates that this linear TENG, as a sensing unit, combined with a signal receiver and microcontroller, can constitute a novel self-powered wearable keyboard. The flexible single-wire TENG introduced in this study had the characteristics of a simple structure, low cost, and high flexibility, and it provides a reference for the application of smart sensing gloves and wearable devices.

Zhao et al.[172] proposed a textile-structured TENG for pressure sensing. As shown in Fig. 4d, this textile-structured pressure sensor used commercial PAN yarn as the substrate and a polymer-assisted metal delamination method (PAMD) to prepare the Cu-PAN yarn. In the PAMD fabrication process, PAN yarns were modified with a thin layer of poly-[(2-(methacryloyl oxy) ethyl) trimethylammonium chloride] (PMETAC), followed by loading of a catalytic palladium salt on the quaternary ammonium groups of PMETAC. After the chemical deposition of copper, the modified PAN yarn was coated with 300 nm copper to obtain a copper PAN yarn. This type of yarn has low resistance and excellent conductivity. Fig. 4e shows a schematic of the pressure sensor woven via knitting. Fig. 4f shows the voltage changes in the knitted textile pressure sensor at different pressures. Through linear fitting, although the sensitivity of the fabric pressure sensor was divided into three different sensing intervals, each interval showed a linear relationship of 0.071 V/kPa and 0.008 V/kPa. Fig. 4g shows a smart glove woven with a yarn. When wearing a glove to grab an object, the sensing unit on the glove generates different voltage signals. The corresponding sensing unit output-pressure distribution was obtained according to the voltage–pressure characteristic curve.

Different programming structures also result in different voltage-output effects. He et al.[173] designed a flexible, stretchable, and wearable fabric-based TENG for the real-time monitoring and display of physiological signals. The structure of a single wire in the fabric is shown in Fig. 4h. This fabric used a spirally wound metal copper spring as the electrode and ZnS:Cu/PDMS coating material as the triboelectric layer. Fig. 4i shows the braided structure of this fabric-type TENG, which could be woven into a flexible fabric. As shown in Fig. 4j, when TENG with braided structure was used as the pressure sensor, it had linear sensitivity of 1.02 V/N and 0.15 V/N in two pressure sensitive regions. In the two intervals, although the rate of change was different, the linear relationship between the output voltage signal and the change in the applied external force was maintained, thereby providing good stability for the sensing function. Fig. 4k shows that the TENG sensor was placed at the finger joint. The voltage signal of sensor also showed a stable difference at different bending angles of the finger joint. The flexible wearable self-powered sensor reported in this paper has broad prospects for applications in the field of human motion monitoring. Pyo, Guan, and Bai et al.[174–176] also adopted a fabric-type TENG as a flexible pressure sensor, which also showed a stable linear sensitivity value.

Metal materials are the most widely used electrode materials because of their excellent conductivity. The unique characteristics of different metals, such as ductility and durability, are highlighted when they adapt to application environments. Copper has the characteristics of soft texture and ductility, and can be prepared into soft copper wire. The copper wire can be made into flexible electrode by multiple knitting methods, which provides excellent electrode material for e-skin manufacturing. Silver also has great ductility. Silver can be prepared into micron and nanometer electrode materials by micro-treatment process. AgNWs is one of the most representative materials. The outstanding performance of metal materials indicates the main direction of further research on the processing and application of metal materials in the future.

3.2. Triboelectric pressure sensor based on a semiconductor electrode material

Among the elements in nature, carbon is an important and widely used non-metallic element. The variability of the covalent bonds between the carbon atoms enables carbon to form a wide variety of allotropes. These can usually be classified according to the dimensions; the representative structures under different dimensions are listed in Table 1. Different carbon allotropes exhibit different properties. Among them, carbon nanotubes (CNT), graphene, and graphene oxide have considerable electrical conductivity. Based on this characteristic, it can be used as a conductor material for TENG with excellent performance [177–179].

3.2.1. Carbon nanotube (CNT) electrode material

To improve sensor flexibility and biocompatibility, Fang et al.[180] proposed a textile triboelectric sensor for cardiovascular health monitoring. Fig. 5a depicts its basic composition. The PMDS layer acted as an attached side encapsulation layer and the outside textile acted as a waterproof protection layer. In the internal structure, the aluminium film and CNT layers served as electrode layers, and the FEP layer served as a triboelectric layer. The CNT conductive network is a monodispersed CNTs deposited on hierarchically structured cotton using a scalable spray-coating method, as shown in Fig. 5b. Therefore, the CNT layer can combine the flexibility and ductility of the yarn-knitted structure with a high electrical conductivity. Fig. 5c demonstrates that this textile triboelectric sensor has a sensitivity of 0.21 μA/kPa and good linearity in the low-pressure operating range 10–40 Pa. Fig. 5d shows the subsequent processing of the sensor signals. The data connection between the Bluetooth module and the designed monitoring APP can be established to monitor cardiovascular characteristics in real time on the mobile terminal of the mobile APP. This study represents a significant milestone for triboelectric sensors in IoT applications.

In the triboelectric sensors used in human–computer interaction equipment, the use of CNT makes the performance of the sensor more stable. The flexible, self-powered keyboard was created by Abdelsalam Ahmed et al.[181] using urethane, silicone rubber, and CNT electrodes. Fig. 5e shows a schematic of a self-powered-keyboard sensing unit, where a layer of air gap and two layers of CNT electrodes on copper tapes constituted the middle portion. Fig. 5f shows the experimental results of the pressure sensing; it can be concluded that the pressure sensitivity of the pressure sensor was divided into two regions of linear variation. In the low- and high-voltage regions, linear variation characteristics of 1.52 mV/Pa and 1.073 mV/Pa were achieved, respectively. Fig. 5g shows that the self-powered keyboard can input information to the computer with the help of an infrared transmitter and receiver connected to the microcontroller. This self-powered flexible keyboard has broad application prospects in wearable electronic devices and

Table 1
Representative structures under different dimensions.

0D	1D	2D	3D
Fullerene	Single-walled carbon nanotubes	Graphene	Diamond
Carbon dots	Multi-walled carbon nanotubes	Graphene oxide	Pillared graphene
Graphene dots	Carbon nanohorns	Multi-layered graphitic sheets	Graphite

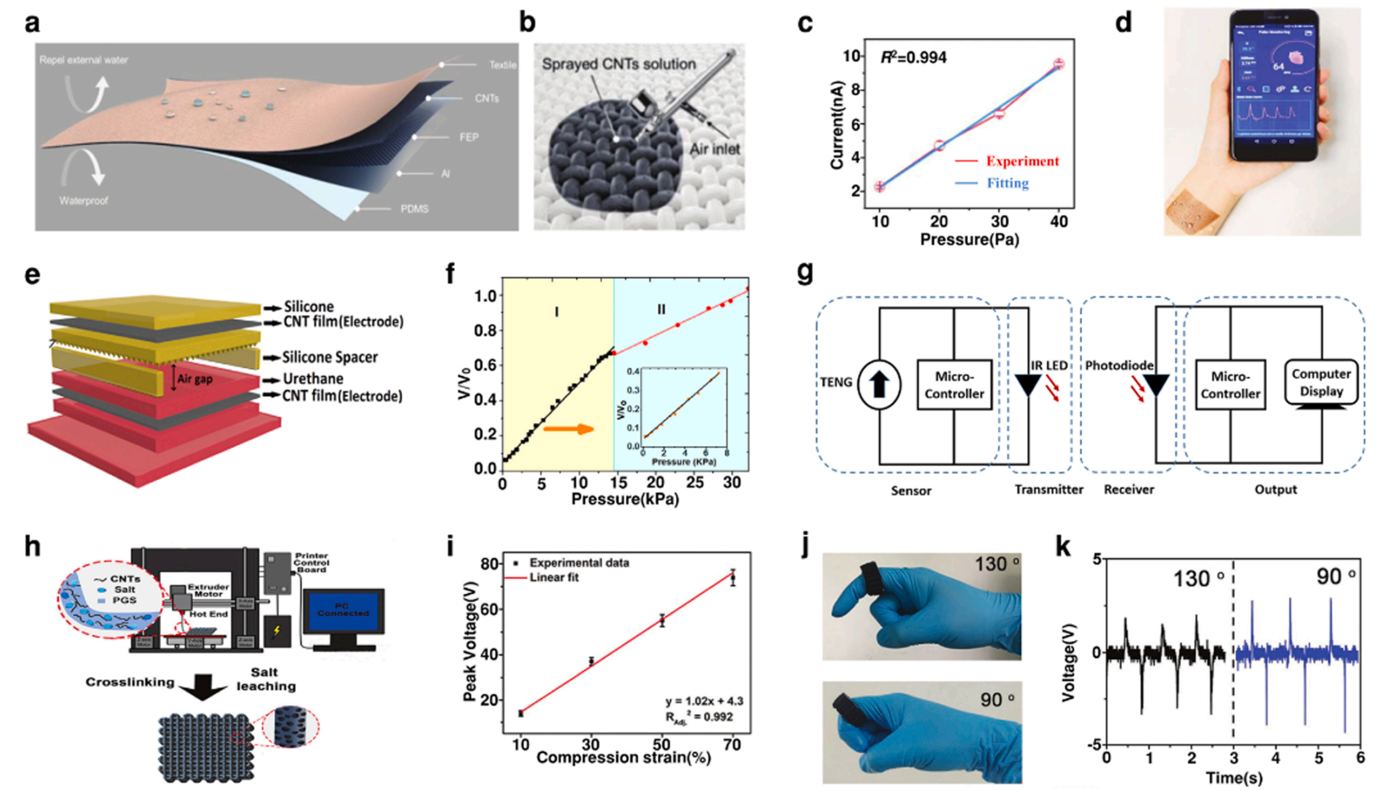

Fig. 5. Carbon nanotube (CNT) electrode material. (a) Schematic of a textile triboelectric sensor. (b) Spray-coating monodispersed CNT solution onto cotton textile to form a conductive network (c) Sensitivity of textile triboelectric sensor. (d) Photograph of the harsh environment tolerant textile triboelectric sensor-enabled real-time pulse monitoring using a mobile phone. (e) Structural design of a flexible TENG keyboard. (f) Relationship and linear fitting between $\Delta V/V_0$ versus applied pressure. (g) Circuit diagram of the self-powered wireless sensing system enabled by keyboard typing. (h) Schematic of the fabrication of a 3D printing TENG (3DP-TENG) and a hierarchical porous structure. (i) Linear dependence of the peak output voltage on different compression strains. (j) 3DP-TENG applied to knuckle bending angle sensing. (k) Different output voltage profiles of the 3DP-TENG during cyclic finger bending at different angles.
(a-d) Reproduced with permission [180] (Copyright 2021, Wiley-VCH). (e-g) Reproduced with permission [181] (Copyright 2017, Elsevier). (h-k) Reproduced with permission [182] (Copyright 2018, Wiley-VCH).

displays, e-skins, and robotic sensing.

Fibres made by mixing CNT with other substances exhibit good conductivity. Chen et al.[182] developed a single-electrode pattern--based TENG sensor using 3D printing technology to monitor limb movements. A schematic of the fabrication of the (3DP-TENG) is shown in Fig. 5h. The main production process involves adding CNTs and salt particles to the PGS to prepare the printing ink. Through the thermal curing process, the extruded paste composite ink could be cured quickly to form a 3D structure. The experimental results presented in Fig. 5i show that the output voltage changes linearly with the compressive strain. This linear characteristic can be used for real-time monitoring and evaluation of the human motion states. Fig. 5j illustrates the 3DP-TENG used for sensing the knuckle-bending angle. Fig. 5k shows the various voltage signals produced by the sensor at various angles corresponding to knuckle-bending angles of 90° and 130°. This TENG with a 3D printed structure can be applied to wearable devices, intelligent robots, and the IoT in the future. Yu and Yang et al.[125,183] also adopted triboelectric pressure sensors with CNT as the electrode material and achieved excellent experimental results. Additionally, both triboelectric pressure sensors exhibited excellent extensibility and hydrophobicity.

3.2.2. Graphene electrode material

Graphene is widely used in electrical devices and structures. In a graphene monolayer, each carbon atom is covalently bonded to nearby atoms to form a honeycomb lattice. This robust structure endows graphene with flexible mechanical properties and impermeability. Furthermore, the physical properties of graphene include its excellent thermal and electrical conductivity. Graphene plays a unique role as a practical, conductive, scalable, and cost-effective material in TENG electrodes.

Lee et al.[184] designed a stretchable TENG (S-TENG) with an ultrathin mesh structure that can be attached to the body parts as a wearable device. Fig. 6a shows the main structure of the S-TENG, which comprised of stacks of PET, bilayer graphene, and polydimethylsiloxane (PDMS) fabricated using a coating process. PDMS was used as the triboelectric layer, and two layers of graphene were used as the electrodes. Fig. 6b shows the variation in the voltage output of the S-TENG at different pressures. It can be seen from the figure that in the pressure range 10.6–101.7 kPa, the voltage–pressure change is a linear trend, and its sensitivity is 0.274 V/kPa. In the trajectory perception experiment, after both the filter procedure and the sensor traversed the ‘2′ shape track, the voltage feedback of each sensing unit exhibited a ‘2′ shape, as shown in Fig. 6c, where the S-TENG, as a wearable sensing device, shows potential as a self-powered wearable communication system device after matching it with a switching multimeter, filter, and other equipments (Fig. 6d). The results of this study can facilitate the realisation of communication and interaction functions in wearable electronic devices that directly send signals and commands.

The performance of a graphene sensor can be improved by changing the 3D structure of graphene. Chen et al. [128] developed a flexible TENG sensor using a crushed graphene (CG) layer. The fabrication process flow of CG is illustrated in Fig. 6e. First, planar graphene was transferred onto a stamp film. After etching, the planar graphene was transferred to a biaxially pre-trained tape. During the relaxation process, planar graphene that was transferred on the tape contracted along with

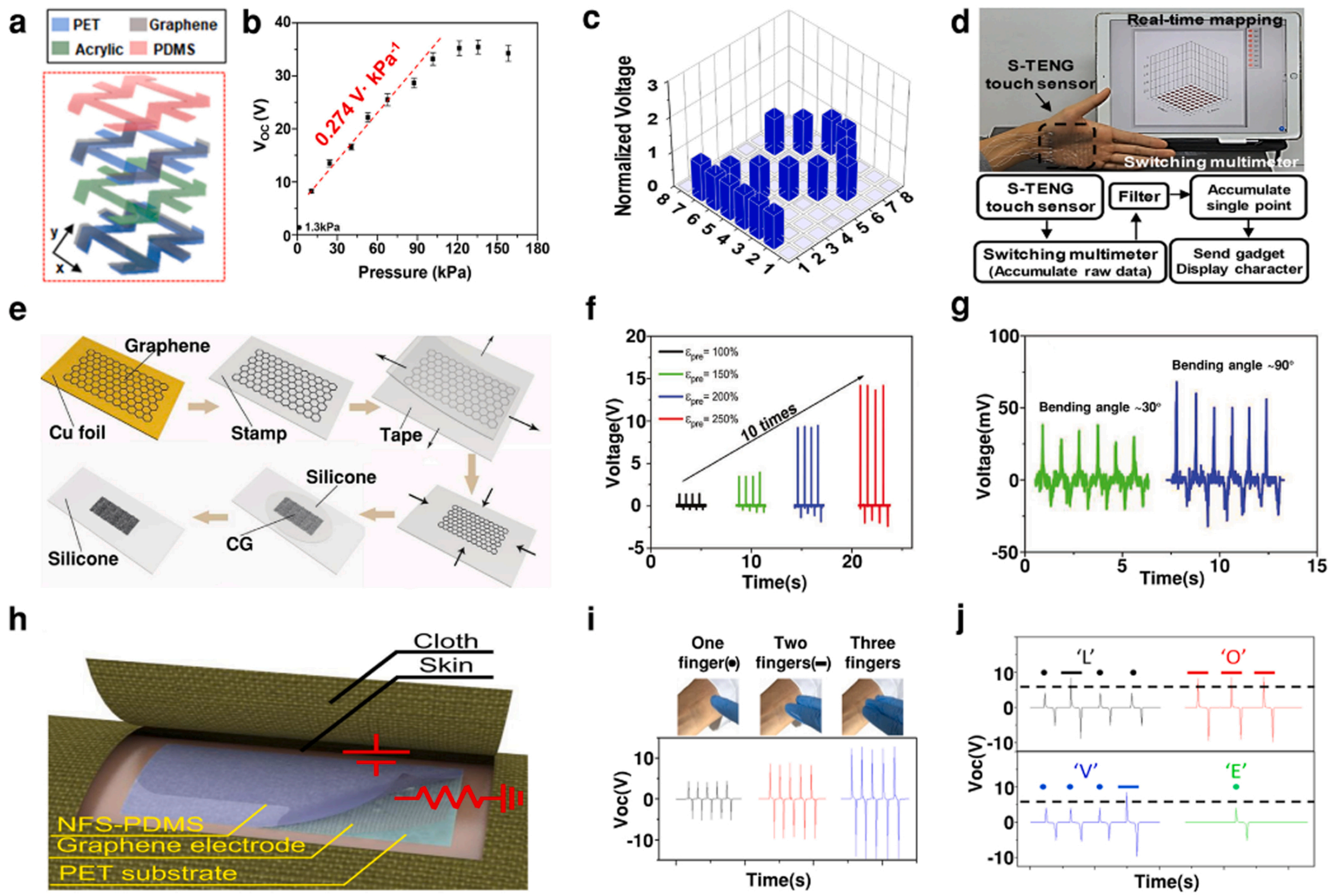

Fig. 6. Graphene electrode material (a) Structure of a self-powered stretchable TENG (S-TENG) touch sensor. (b) Sensitivity of S-TENG. (c) Results in a trajectory mode. (d) Real-time mapping trajectory mode to which the logical filter process, (e) Schematic of the fabrication process flow of crumpled graphene (CG). (f) Output voltages of TENGs with different ε_{pre} values. (g) Real-time voltage changes for finger bending at two different angle. (h) Schematic of the conformal TENGs formed on human skin. (i) Voltage output of the self-powered contact sensors in contact with the different number of fingers. (j) V_{OC} of the four different sequences corresponding 'L′, 'O′, 'V′, and 'E′.
(a-d) Reproduced with permission [184] (Copyright 2019, Elsevier). (e-g) Reproduced with permission [128] (Copyright 2017, Wiley-VCH). (h-j) Reproduced with permission [185] (Copyright 2016, Elsevier).

the tape and was crumpled. Fig. 6f shows the results of the study on the effect of different degrees of wrinkles on the output voltage. Its output voltage was an order of magnitude higher than that of the TENG composed of planar graphene layers in the control experiment. When CG-TENG was used as a sensor, different voltage signals were generated for different bending angles of the knuckles (Fig. 6g), thereby realising the human motion monitoring functions. This CG-TENG provides a new concept for future applications in wearable devices and embedded sensors.

The application of graphene in human skin sensing has also shown excellent performance. Chu et al. [185]reported that an ultrathin TENG sensor could be attached to the human skin, and its main structure is shown in Fig. 6h, with a nanostructured and functionalized surface (NFS), called NFS-PDMS, as the contact triboelectric layer, a graphene layer as the electrode layer, and a PET film as the encapsulation layer. Fig. 6i shows that when used as a wearable device, it can generate different voltage signals when different numbers of fingers are pressed. According to this characteristic and with the help of signal processing and transmission equipment, the voltage signal can be converted into a Morse code to realise information exchange (Fig. 6j). This study extended the use of TENG sensing technology in areas such as human–machine interface interaction. Yang and Liu et al.[44,186] used graphene as the sensor electrode material to fabricate a flexible triboelectric sensor and achieved excellent results.

In addition to the aforementioned TENGs based on graphene electrodes fabricated through relatively simple processes, there are more production and processing processes for graphene electrodes. In one of these processes, graphene oxide is modified using a chemical oxidation process. Graphene oxide is amphiphilic and exhibits a distribution of hydrophilic to hydrophobic properties from the edge to the centre of the graphene flakes.

Based on this property, Wu et al.[134] developed a liquid single-electrode TENG (LS-TENG) based on graphene oxide dispersion (GO LS-TENG) with high flexibility, deformability, and good mechanical properties. The LS-TENG used graphene oxide (GO) dispersions as liquid electrodes and flexible PDMS as triboelectric layers. The manufacturing process is illustrated in Fig. 7a. First, PDMS was poured into a pre-assembled aluminum plate as a mould for post-curing. The GO dispersion was then coated inside two PDMS films. Fig. 7b clearly shows that the GO LS-TENG produced opposite voltage signals when the skin exerted and removed pressure. As shown in Fig. 7c, the GO LS-TENG was used as a skin sensor, which has a high sensitivity to tiny contact movements, such as finger contact. The high sensitivity of the GO LS-TENG has potential application as a body-motion state sensor and e-skin. He, Wu, and Guo et al.[135,136,187] also conducted a study of graphene oxide as an electrode material.

In addition to the chemical modification process, the laser direct writing (LDW) technique can be used to produce highly conductive porous graphene in wood, cloth, and paper[188,189]. Yan et al.[133] proposed a facile and efficient general-purpose LDW technique for the

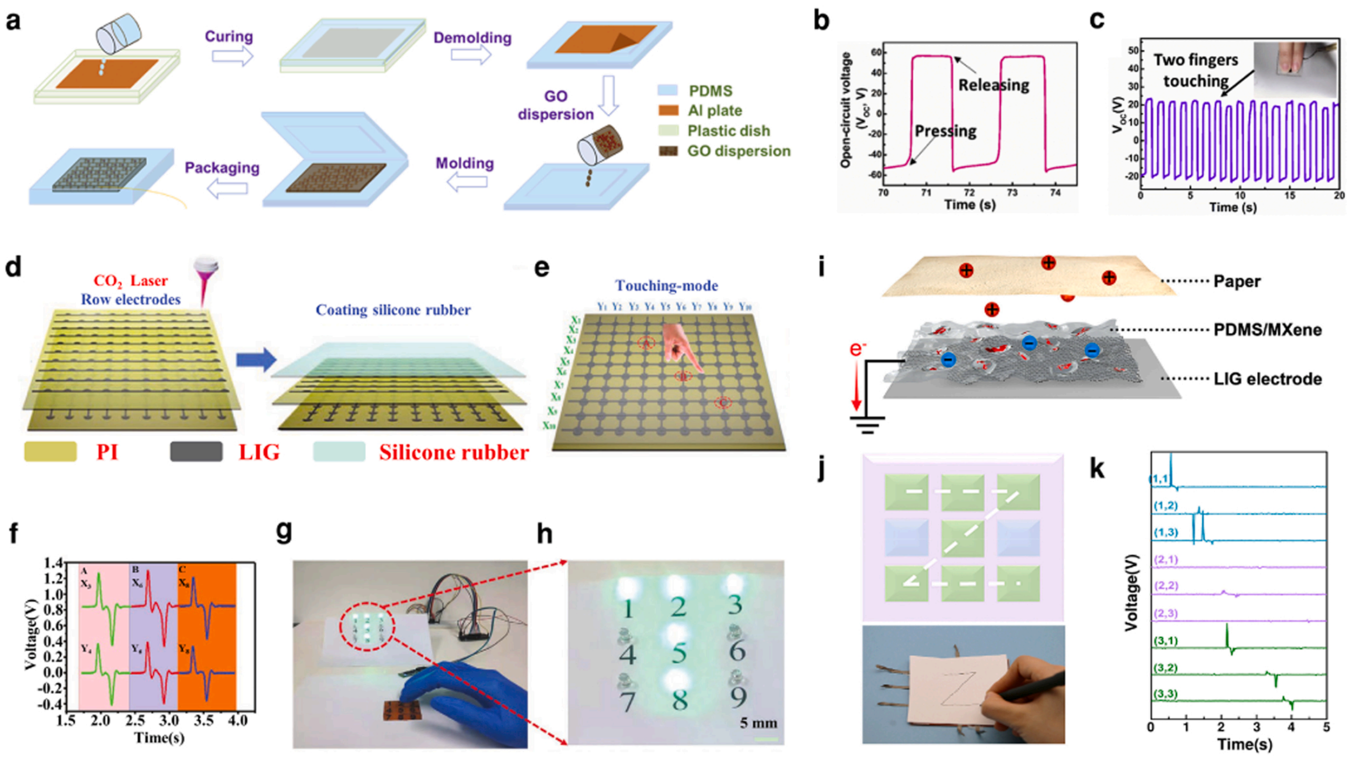

Fig. 7. Graphene oxide and laser-induced graphene. (a) Fabrication process of a liquid single-electrode TENG (LS-TENG) based on graphene oxide dispersion (GO LS-TENG). (b) Open-circuit voltage levels when performing the pressing and releasing operations. (c) Output V_{OC} of GO LS-TENG when two fingers perform the touching and releasing operations. (d) Schematic of fabrication process of triboelectric sensing array (TSA). (e) Multi-point touch mode. (f) Output voltages of pixels when being touched. (g) LED that is wirelessly controlled by the human–machine interactions (HMI) system. (h) Enlarged photograph of the LED. (i) Structural diagram of a TENG used for human writing process. (j) Z-shaped writing path. (k) Measured voltage signals.
(a-c) Reproduced with permission [134] (Copyright 2019, Elsevier). (d-h) Reproduced with permission [133] (Copyright 2021, Elsevier). (i-k) Reproduced with permission [131] (Copyright 2019, Elsevier).

fabrication of patterned laser-induced graphene (LIG) electrodes. Based on this technique, they designed a flexible triboelectric sensing array (TSA) for tactile sensing. The structure and fabrication method are illustrated in Fig. 7d. TSA is composed of silicone rubber as a protective and triboelectric layer and two laminated LIG-embedded PI films, produced using precisely programmable LDW. The two semi-circular array electrode layers overlapped in a reverse complementary manner. Figs. 7e and 7f demonstrate the stable performance of the TSA for multi-touch sensing. Fig. 7g and 7h show the TSA as a self-powered sensor, where the sensor voltage signal was passed through a micro-controller and wireless Bluetooth module, demonstrating the ability of the TSA as a smart wireless control and self-powered sensor. In this study, the TENG based on the LIG-patterned electrodes provided a reference for building self-powered wireless control systems and real-time tactile sensing systems. The application of laser direct writing technology has considerably improved the stability of sensors, which also makes LDW technology favoured by more researchers.

Jiang et al.[131] developed a highly flexible TENG based on an MXene and polydimethylsiloxane (PDMS) composite (PDMS/MXene) film and an LIG electrode, and its structural diagram is shown in Fig. 7i, with the porous PDMS/MXene film as the triboelectric layer. To fabricate highly flexible LIG electrodes, a convenient laser-induced technique was applied, and it prepared 3D porous multi-layer graphene on a PI substrate at room temperature. After arranging the TENGs in an array, the track information was identified according to the signal generation sequence of each sensing unit. Fig. 7j shows that as a writable sensor, when a ‘Z’-shaped track is drawn on the TENG, similar to drawing on a paper, the corresponding voltage signals were obtained by measuring different sensor units (as shown in Fig. 7k). Wang and Tao et al.[190, 191] also applied LDW technology to fabricate patterned electrodes.

Carbonaceous nanomaterials are widely used in triboelectric pressure sensors for the merits of high conductivity, rich forms and derivatives. Carbonaceous nanomaterials have superior oxidation resistance compared with metals, which makes them more suitable for electrode materials of sensors in oxidizing environments. CNT is a reliable material to improve sensing performance with low difficulty. CNT can be manufactured as an electrode by most technology like coating and spraying. Graphene not only has excellent conductivity and oxidation resistance, but also has high transparency and flexibility. Therefore, graphene is the optimum electrode material for e-skin. Graphene oxide has more advantages like largescale production and easy processing compared to graphene, which are of great significance for the wide use of graphene oxide in the future.

3.3. *Triboelectric pressure sensor based on hybrid electrode materials*

The use of hybrid electrode materials to improve the physical properties of electrode materials or to improve the voltage signal output of TENGs is in great demand for research in recent years.

3.3.1. *Conductor and semiconductor hybrid electrodes*

Innovative selection and processing technologies have been developed and extensively studied for hybrid electrodes of conductors and semiconductors. Zhou et al.[192] reported a e-skin based on ultra-stretchable triboelectric nanogenerator (STENG) and simultaneously designed a conductive network of redox graphene (rGO) combined with AgNWs in a multilayer flexible structure. Fig. 8a shows the fabrication process of the conductive network of rGO combined with the AgNWs, where rGO was sonicated for 1 h and then dispersed in ethanol. AgNWs stored in ethanol were uniformly mixed with the rGO dispersion

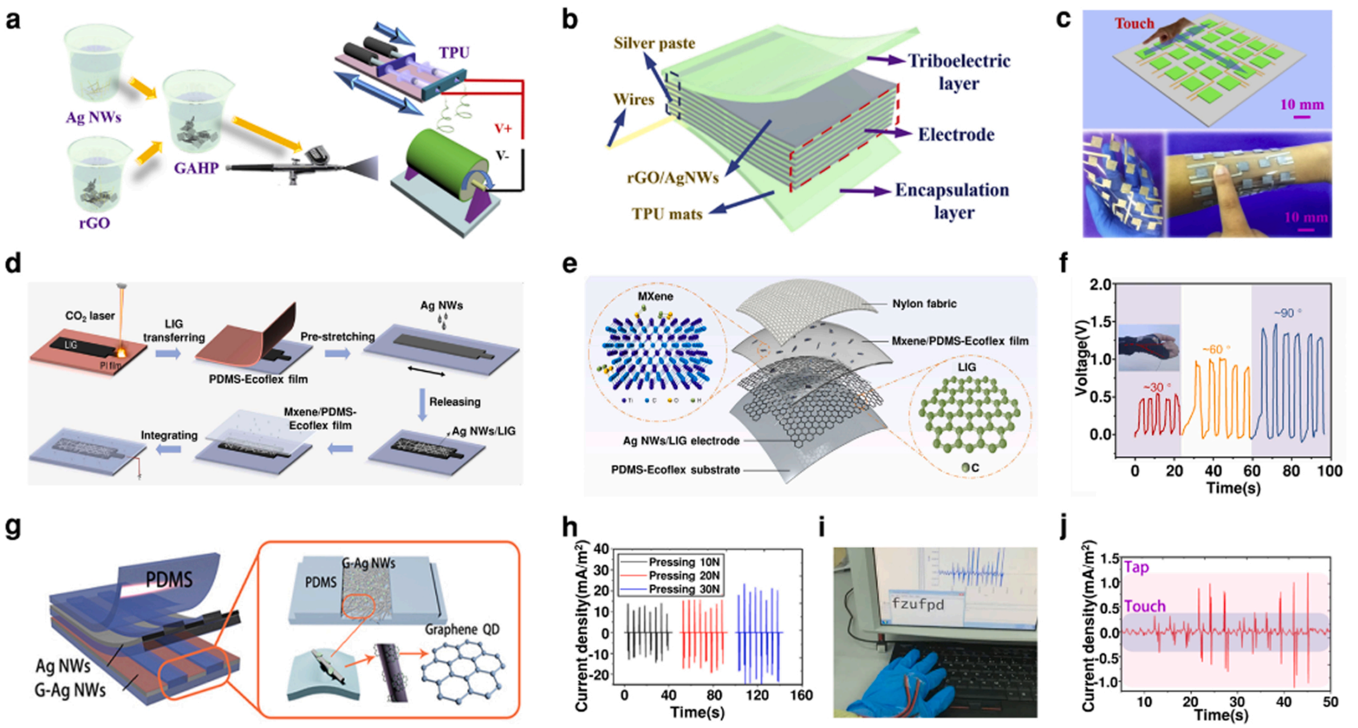

Fig. 8. Conductor and semiconductor hybrid electrodes. (a) Schematics of the preparation process and equipment for fabricating an e-skin. (b) Schematic of an e-skin structure. (c) Schematic of a flexible tactile sensing e-skin array. (d) Process flow diagram of the stretchable porous MXene/LIG foam-based TENG preparation. (e) Schematic of the MXene/LIG foam-based TENG structure. (f) Output from the self-power strain sensor at various wrist-bending angles. (g) Schematics of the e-skin and graphene quantum dot-coated AgNW (G-AgNW) network. (h) Short-circuit current density output for the e-skin with graphene QDs when the e-skin is pressed. (i) Photograph of a keyboard being tapped with smart artificial fingers. (j) Time evolution of the current density when the index finger touches and taps a key. (a-c) Reproduced with permission [192] (Copyright 2020, Elsevier). (d-f) Reproduced with permission [193] (Copyright 2022, Elsevier). (g-j) Reproduced with permission [93] (Copyright 2018, Elsevier).

after high-speed stirring. Finally, the mixed solution of rGO and AgNWs was uniformly attached to the thermoplastic polyurethane (TPU) fibre mat by spraying. Fig. 8b shows the e-skin based on STENG. The overall structure comprised nine layers of TPU and eight layers of rGO and AgNW conductive layers. The top TPU served as the triboelectric and protective layers, and the bottom TPU material served as the encapsulation layer. The conductive layer of the multilayer structure improved the stretchability and flexibility of the e-skin while providing triboelectric output performance. In practical applications, multiple single sensing units are integrated to form a wearable self-powered e-skin array that realises the functions of finger-touch mapping feedback, as shown in Fig. 8c. The results show that the e-skin in this study is capable of skin touch trajectory sensing, reflecting the potential application value of TENG sensors in human–computer interaction.

The method for forming a mixture before processing was adopted in the aforementioned study. Different materials can be processed individually using different processing technologies. Yang et al.[193] presented a fully stretchable TENG consisting of an intrinsically stretchable MXene/silicone elastomer and AgNW graphene foam nanocomposite. The fabrication process of AgNW graphene foam nanocomposite is shown in Fig. 8d. First, 3D porous LIG foam electrodes were fabricated by direct laser heating of a 75 μm-thick PI film. After transferring the LIG electrode onto the flexible silicone rubber substrate, pre-straining, and spraying AgNW solution on the pre-stretched LIG/PDMS-Ecoflex electrode, a stretchable AgNWs/LIG electrode was prepared by releasing the pre-strain. An exploded structural view of the fabricated TENG is shown in Fig. 8e. The top nylon layer and bottom PDMS-Ecoflex composite film were used as the encapsulation layer, the MXene/PDMS-Ecoflex composite film was used as the triboelectric layer, and the porous Ag NWs/LIG composite was used as the electrode layer. When the TENG with this structure was used as a sensor for the human joint motion-sensing function, as shown in Fig. 8f, the output electrical signal of the TENG produced stability differences corresponding to the different joint-bending angles. When used as a self-powered sensor attached to the human skin, it could adapt to the bending changes to the joints in different parts and perform real-time motion monitoring. This is a solid step in the application of TENGs as self-powered biological sensors.

Similarly, Xu et al.[93] adopted successive processing, where they designed a transparent and stretchable e-skin. This e-skin used AgNWs coated with graphene quantum dots as the electrode layer, and its structure is shown in Fig. 8g. The fabrication process of the electrode layer is to treat PDMS and AgNWs with oxygen plasma first to increase hydrophilicity. Then, the AgNWs were deposited on the PDMS layer, and the graphene quantum dots were blade-coated on the surface of the AgNW film and annealed at 90 °C for 20 min. Finally, the graphene quantum dots were attached to the silver nanowires via van der Waals forces. Fig. 8h shows an obvious difference in the current generated by the sensor under different external pressure excitations. Based on the variability of the current, it is possible to record the contact and pressing actions of the fingers when using different degrees of pressing buttons on e-skins. This study should have a high reference value for future studies on e-skin, and prosthetic sensing. Li and Chen et al.[194,195] also used conductor and semiconductor hybrid electrodes to fabricate triboelectric sensors with excellent performance.

3.3.2. *Conductor/semiconductor and polymer hybrid electrode materials*

Conductor/semiconductor and polymer hybrid materials, have good conductivity and electronegativity. Wang et al.[138] designed a self-powered triboelectric tactile sensor with polydimethylsiloxane (PDMS) as the triboelectric layer and PDMS/eutectic gallium indium (EGaIn) alloy as the composite electrode. The sensor is characterised by a simple manufacturing process and low cost. Fig. 9a shows the fabrication process flow of this TENG. First, the multi-layer structure and wrinkle structure of sandpaper were used as the mould, effectively improving the surface roughness and contact area of the triboelectric layer PDMS. The high electrical conductivity of the PDMS/EGaln composite electrode material improves the triboelectric output performance. Fig. 9b shows a schematic of the working principle of the pressure sensor. The working cycle process of the TENG was realised through the application and release of an external force. Fig. 9c shows the linear relationship between the output voltage of the triboelectric sensor and the applied external force in the experimental test results. It can be seen from the figure that the TENG sensor maintained stable sensitivities of 0.293 mV/Pa and 0.103 mV/Pa in the pressure ranges of 0.23–13.12 kPa and 13.12–95.95 kPa, respectively. According to the different pressure sensitivities of the two intervals, the voltage signals were processed and used for the detection of the human pulse physiological signal (Fig. 9d). This composite self-powered triboelectric tactile sensor, with an ultra-low detection limit and high sensitivity, provides a new reference for the development of next-generation electronic devices.

Successive moulding process has the characteristics of a simple structure and simple manufacturing. However, more sophisticated processing technologies can significantly improve the performance stability of hybrid electrode materials. Wang et al.[121] introduced a self-powered triboelectric tactile sensor (TETS) that used Ag nanofibres (AgNFs) as electrodes. The fabrication process of the AgNFs is shown in Fig. 9e. First, by changing the shape of the metal collector during the electrospinning process, different types of polyvinyl alcohol nanofibres (PVA NFs) with controllable orientations were obtained. A thin layer of silver was then deposited on the surface of the PVA NFs by magnetron sputtering. Finally, nanofibres with a PVA/Ag core/shell structure were formed, and this composite fibre had excellent electrical conductivity. The layered structure of the TENG is shown in Fig. 9f, which consists of the PDMS electrification layer, row AgNF electrode, PDMS insulator layer, column AgNF electrode, and bottom PDMS substrate from top to bottom. Fig. 9g shows that after the sensor array was made, the multi-channel data acquisition system was used to realise the function of touch point positioning. Therefore, when the continuous track touches the sensor array, the track feedback function, as shown in Fig. 9h, can be realized. The single-electrode tactile sensor in this study realises the tactile mapping feedback function, which provides a new concept for the application of self-powered sensors in wearable devices and smart touchpads. Hybrid electrodes of semiconductor and polymer materials also exhibit excellent performance.

Peng et al.[29] used co-extrusion blow film moulding technology to prepare a large-area sandwich-film-based TENG (LSF-TENG). The sandwich structure of the LSF-TENG consists of upper and lower layers of PP and carbon nanotubes compounded with a CNTs/PP phase in the middle. Fig. 9i shows the fabrication process diagram of CNTs/PP. The dried PP particles were mixed with CNTs, and the CNT/PP particles were extruded through an extruder (extruder). The LSF-TENG was prepared by blowing particles into a tubular film through a co-extrusion blow film moulding method. Fig. 9j shows that the LSF-TENG was cut into strips (4 mm × 50 mm) for the self-powered biomimetic whiskers(SPBWs). When SPBWs slide across a surface with continuous grooves, the voltage signal generated by a weak disturbance is collected by the acquisition card and displayed on the computer in real time. Subsequently, according to the number of voltage signal peaks at a certain time, the distance and speed of movement can be obtained. According to this

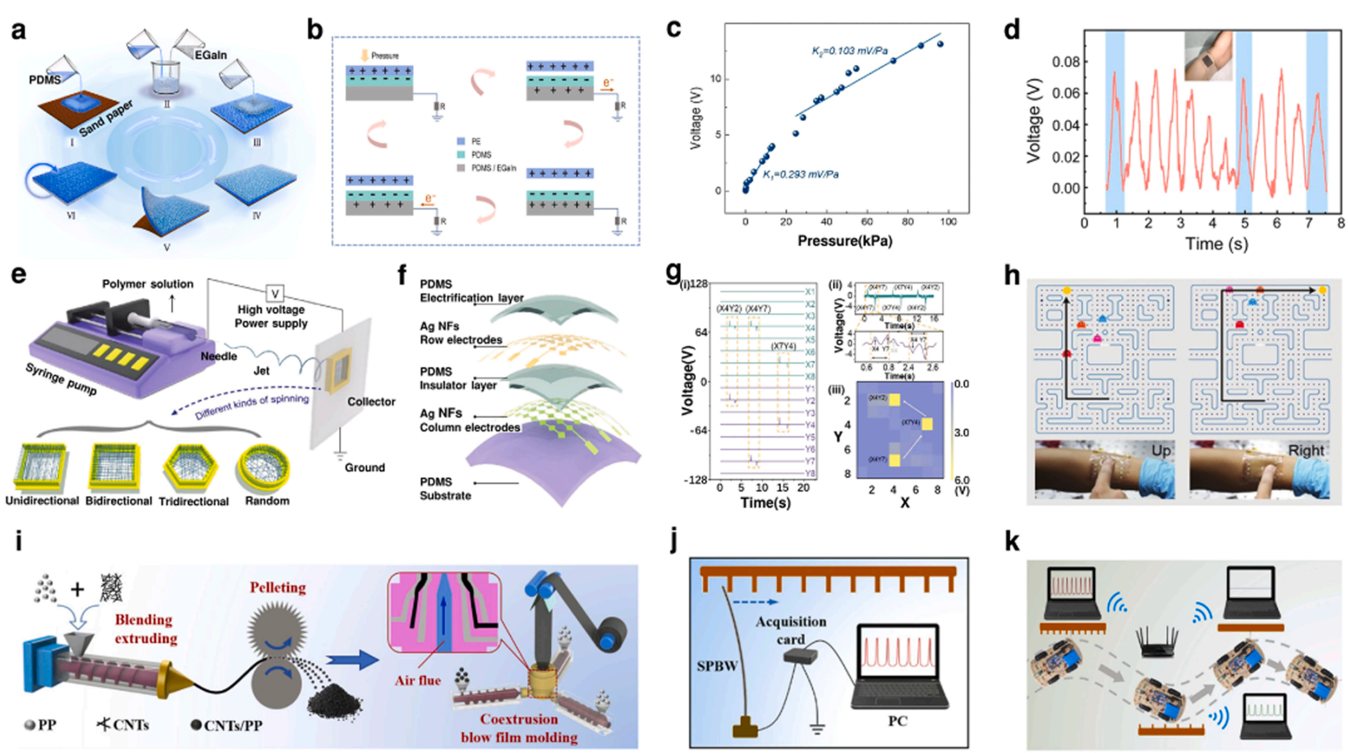

Fig. 9. Conductor/Semiconductor and Polymer Hybrid Electrode Materials. (a) Fabrication process of self-powered triboelectric tactile sensor with PDMS/EGaIn alloy electrode. (b) Fundamental working mechanism of self-powered triboelectric tactile sensor. (c) The sensitivities of the tactile sensor in the whole testing pressure range, (d) The stretchable self-powered triboelectric tactile sensor attached to the wrist of the human subject. (e) Schematic illustration of the electrospinning with different collectors to obtain various PVA NFs with controlled fiber orientation. (f) Schematic structure of the TENG. (g) The multi-channel data acquisition system is used to realize the function of touch point positioning. (h) When the continuous track touches the sensor array, the track feedback function can be realized. (i) Schematic fabrication of a large-area sandwich-film-based TENG(LSF-TENG). (j) LSF-TENG is used for self-powered biomimetic whiskers (SPBWs). (k) Schematic diagram of the process of automated guidance.

(a-d) Reproduced with permission [138] (Copyright 2018, Wiley-VCH). (e-h) Reproduced with permission [121] (Copyright 2020, Elsevier). (i-k) Reproduced with permission [29] (Copyright 2022, Elsevier).

function, the process of automatic guiding and motion state monitoring of a smart car can be realised (Fig. 9k). In future research, automatic obstacle avoidance driving of the car and texture recognition feedback of the contact surface can also be realised. The sensitive tactile perception of SPBWs is an important technical reference for subsequent self-powered tactile perception technology. Rasel and Zhao et al.[85, 196] also used a hybrid electrode of a semiconductor and polymer material as the electrode material of the triboelectric sensor.

Hybrid electrode materials made of two or more different types of materials can often integrate the advantages of various materials to improve the comprehensive performance. Most hybrid electrode materials have the characteristics of high conductivity, flexibility and ductility. However, the more types of materials involved, the more complex the manufacturing process of hybrid electrode materials.

3.4. Gel electrode materials

Gel electrode materials have been widely studied in recent years. Gel electrode materials include ionic gel and hydrogel, which are mainly used in human health perception and e-skin.

Gel materials include hydrogels and ionogels. They exhibit good biocompatibility and are widely used in the manufacture of human skin sensors and wearables. Yang et al.[70] reported a flexible stretchable polyvinyl alcohol/phytic acid (PVA/PA) hydrogel for self-powered HMI sensing (Fig.10a-(i)) in an intelligent medical system based on a TENG. The structure of the PVA/PA hydrogel-based TENG (PH-TENG) is shown in Fig.10a-(ii). Ecoflex acts as a triboelectric material and as a sealing material to prevent water loss from hydrogels and is used to encapsulate PVA/PA hydrogel electrodes. Freeze–thaw cycles are a common method for preparing PVA hydrogels because the freezing of PVA and phase separation leading to gelation occur during the process. Therefore, PVA/PA hydrogels were prepared by a one-step freeze–thaw method, as shown in Fig. 10a-(iii). Fig. 10b shows that the triboelectric sensor was fixed to the fingers of both hands. Through multi-signal acquisition, different information content can be conveyed through different gestures. Fig. 10c shows different gesture combinations in which the 'HELP' message was transmitted to correctly express the seeker's needs. This study is expected to develop into an alternative strategy in the field of human–machine interfaces in medical care and can be extended to other fields, showing broad implications in smart flexible electronics and the brain–machine interfaces.

Zhao et al.[44] used another ion gel material in their research. They designed and fabricated a stretchable and highly flexible skin-adaptive self-powered triboelectric sensor that can be used in physiological fields such as tactile sensing and joint limb bending sensing. The structure of this TENG is shown in Fig. 10d; it consists of a transparent stretchable ion gel as electrodes and one triboelectric layer, with micro-patterned PDMS as another triboelectric layer. This triboelectric sensor has strong stretchability and can maintain a good linear relationship between the voltage and pressure under different tensile strains, as shown in Fig. 10e. Therefore, it also shows very good performance when used as a limb joint motion-sensing sensor. Fig. 10f shows the experimental results of the sensor for finger tactile perception and finger joint curvature perception. Evidently, the triboelectric sensor in this study has broad application prospects in the perception of human body movement posture, respiration, and pulse.

In addition to ion gels, the application of hydrogel materials increases the abundance of gel-type triboelectric materials. Lee et al.[145] developed self-cleanable, transparent, and attachable ionic communicators (STAICs) based on TENG. Fig. 10g shows the fabrication process

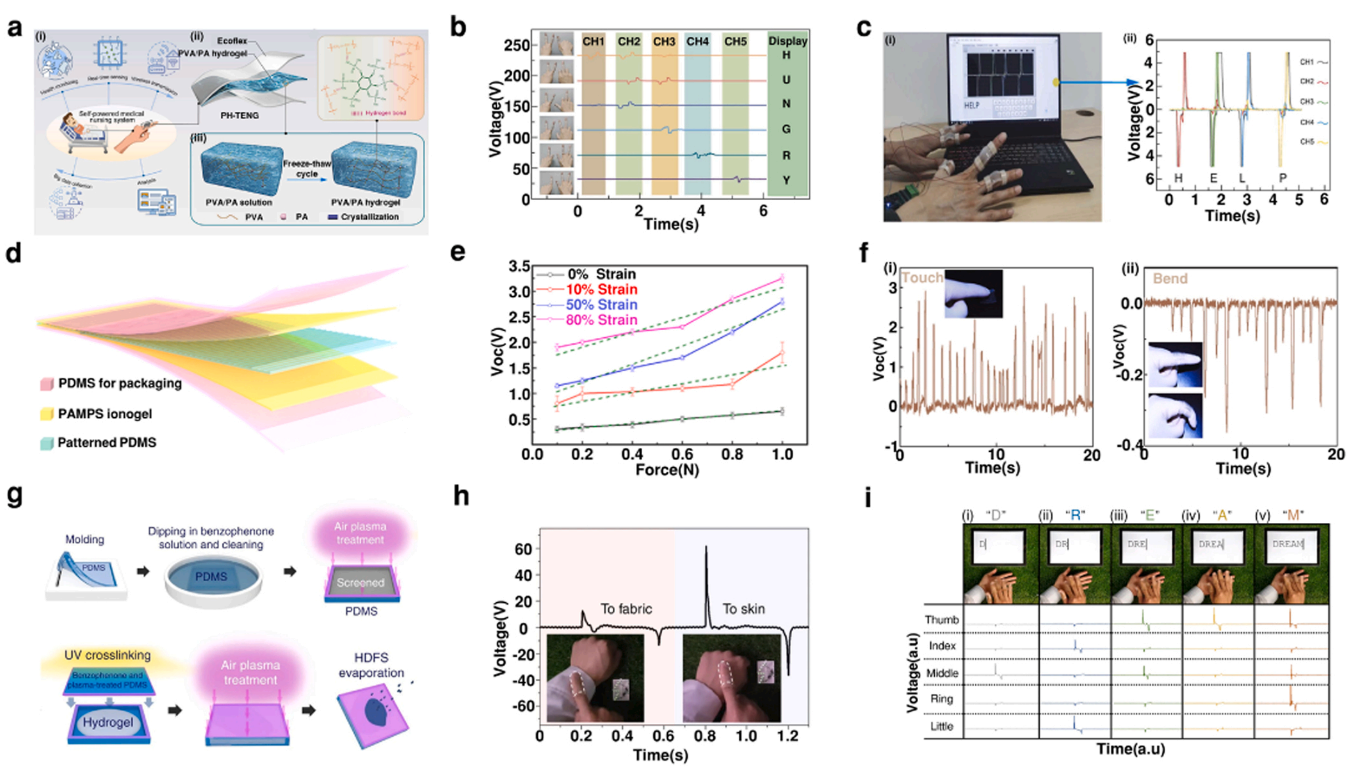

Fig. 10. (a) Overview of a PVA/PA hydrogel-based TENG(PH-TENG) assembled on the finger for health monitoring. (b) The combination of different gestures expresses the word. (c) The word "help" is displayed on the interface of the system. (d) Layered structure of the sensor. (e) V_{OC} of the sensor at different ratios of tension under different force at 1 Hz. (f). The triboelectric signal of the sensor generated by touching and bending. (g) Fabrication process of self-cleanable, transparent, and attachable ionic communicators (STAICs). (h) Generated voltages of a STAIC by a gentle touch to a fabric and the skin. (i) Demonstration of real-time communication with STAICs.
(a-c) Reproduced with permission [70] (Copyright 2022, Elsevier). (d-f) reproduced with permission [44] (Copyright 2019, Elsevier). (g-i) Reproduced with permission [145] (Copyright 2018, Nature Portfolio).

flow of STAICs. The dried and cured PDMS was immersed in 15 wt% ethanol solution of benzophenone for 10 min and washed with methanol to activate the elastomer surface. The hydrogel solution was poured over the activated bottom PDMS layer and covered with the top PDMS layer. The hydrogels formed chemical bonds with PDMS by directly curing the hydrogel precursors onto the benzophenone-absorbing PDMS surface, followed by 365 nm UV irradiation for one hour. A self-assembled monolayer (SAM) was formed using vapour. Pt electrodes were inserted into the hydrogel via encapsulated PDMS to measure the electrical properties of the STAICs. Fig. 10h shows the different voltage signals generated by STAICs as self-powered sensor devices when they touch clothing and skin. Here, the STAICs were attached to fingers, and each finger action combination was designed to correspond to different letter inputs. As shown in Fig. 10i, according to different letters corresponding to different gestures, different gestures can be used to send letter instructions, and the function of information transmission can be realised. As shown in the figure, the researcher successfully completed the input of the word 'DREAM'. Therefore, STAICs can be used as real-time human–computer interaction devices by collecting the gentle touch signals of fingers. The STAIC opens new avenues for wider applications of stretchable ions, soft robotics, and self-powered biomechanical motion monitoring systems. He and Long et al.[197,198] also adopted conductive-gel materials as electrode materials for triboelectric sensors.

Gel electrode materials exhibit excellent stretchability, high transmittance and biocompatibility, making them the significant materials for triboelectric pressure sensors in the field of human-machine interfaces and monitoring systems for biomechanical motion.

4. Summary and perspectives

The selection of electrode materials for the triboelectric sensor, the application of processing technology, and the performance of the sensor in the research work detailed in this paper are summarized in Table 2.

The triboelectric pressure sensors with various electrode materials and electrode structures show different performance characteristics. The triboelectric pressure sensor with conductor electrode material has a wide pressure monitoring range and high sensitivity. However, the electrode with woven fabric structure will sacrifice some sensitivity while improving the flexibility of the electrode. The triboelectric pressure sensor with semiconductor electrode material also has a wide pressure monitoring range. The high-precision processing technology of carbonaceous nanomaterials provides strong support for the stable monitoring sensitivity of the triboelectric pressure sensor. The performance of triboelectric pressure sensor with hybrid electrode materials mainly depends on the type of hybrid electrode materials and processing technology. The hybrid electrode materials prepared by two or more materials can make up the advantages and disadvantages of different materials, and make the electrode materials have multiple performance advantages at the same time. The triboelectric pressure sensors using gel electrode materials have high biocompatibility and extensibility. Therefore, most of the triboelectric pressure sensors using gel electrode materials have different sensitivity at diverse stretching ratios.

Self-powered pressure sensors based on TENGs have been widely used in wearable devices, human–computer interactions, health monitoring, and other fields owing to their advantages of being self-powered and high sensitivity. However, triboelectric pressure sensors still have unresolved issues in terms of material selection, fine manufacturing process of materials, and sensor fabrication costs in different application environments, hindering their development as self-powered pressure sensors in various fields.

By making changes in the selection of materials for fabricating TENGs, selecting electrode materials with the characteristics of a stable electrical signal, high durability, and high adaptability to the application environment can effectively improve practical applicability in some fields. For example, in the application of e-skin and wearable devices, semiconductor materials such as carbon fibre, graphene, and its derivatives have been selected as electrode materials.

Owing to their good conductivity, flexibility, corrosion resistance, and other characteristics, semiconductor electrode materials are the best choice for flexible pressure-sensor electrode materials. It is also possible to improve the sensing accuracy and sensitivity of the TENG pressure sensors by refining the processing technology of the electrode material. For example, for the micro–nano-structure processing of conductor electrode materials, the selection of nano-scale materials, such as AgNWs and CNTs, can provide a highly convenient material selection for the preparation of micro-nano-scale electrode materials.

More number of complex processing technologies that use high-precision instruments and equipment can be used to process the electrode materials. For example, LDW, mask lithography, and other fine processes can not only complete nanoscale processing, but also finely process patterned electrodes with different design requirements. More importantly, the electrode material adopts fine processing technology, which can considerably improve the performance uniformity of multiple sensors of the same type. The main principle is that the surface treatment

Table 2
Summary of Triboelectric Sensor Technology and Characteristics.

Electrode type	Electrode material	Structure/Process	Sensitivity	Monitoring range	Ref.
Conductor electrode	Cu	Array	53.7 mV/Pa 5.3 mV/Pa 1.2 mV/Pa	0.1–0.7kPa 2.5–21.5kPa 25.5–37.5kPa	[47]
	Ag	Array/magnetic sputtering	$0.06kPa^{-1}$	< 80kPa	[84]
	AgNWs	Nanowire	$0.011kPa^{-1}$	< 40kPa	[95]
	Steel	Textile		< 6 N	[171]
	Cu	Textile/PAMD	$0.071VkPa^{-1}$ $,0.008\ VkPa^{-1}$		[172]
	Cu	Textile	$1.02VN^{-1}$, $0.15\ VN^{-1}$	0–5 N 6–45 N	[173]
Semiconductor electrode	CNT	Nanotube	$0.21\ \mu A\ kPa^{-1}$	10–40 Pa	[180]
	CNT	Nanotube	$1.52mVPa^{-1}$, $1.073mVPa^{-1}$	0–13kPa 13–29kPa	[181]
	Graphene	Coating	$0.274VkPA^{-1}$	10.6–101.7kPa	[184]
Hybrid electrode	AgNWs& rGO	Network/ Spraying	$78.4kPa^{-1}$ $16.1kPa^{-1}$	< 5kPa	[192]
	AgNWs& LIG	LDW	-	< 17 N	[193]
	EGaln& PDMS	Molding	$0.293mVPa^{-1}$, $0.103\ mVPa^{-1}$	< 100kPa	[138]
Gel electrode	Ionogel	PAMPS ionogel	$0.378\ VN^{-1}$(0% strain) $0.867\ VN^{-1}$(10% strain) $1.822\ VN^{-1}$(50% strain) $1.444\ VN^{-1}$(80% strain)	-	[44]

of the electrode material by the fine process can keep the surface micro-nano structural properties of the electrode material highly similar, so that the charge distribution on the surface of the electrode material remains uniform. Fig. 11.

The above summary of electrode material selection and treatment processes also reveals the future development direction of electrode materials for triboelectric pressure sensors. The primary development directions include the development of more abundant material types, increased sensitivity, enhanced flexibility, and simplified processes.

4.1. Develop new materials

In a practical application environment, the triboelectric pressure sensor will inevitably face environment complexities such as high humidity, high-frequency friction, and salt corrosion. The abundant selection of electrode materials can provide electrode materials with improved environmental adaptability for triboelectric pressure sensors in various application environments. In previous studies, single materials such as conductors and semiconductors have already exhibited excellent conductivity and durability. However, hybrid-type electrode materials show outstanding flexibility. In the future, the development of new materials will be an important research direction for triboelectric pressure sensors.

4.2. Increase sensitivity

As a type of pressure sensor, triboelectric pressure sensors naturally need to show excellent sensitivity. Therefore, more precise nano-scale and micro-scale processing technologies are required to improve the sensitivity of the sensors. For example, the commonly used 10.2 μm laser direct writing, magnetic pole sputtering, and electrostatic spinning technologies have effectively improved the sensitivity of triboelectric sensors. Therefore, using greater precision processing technologies to process materials is a crucial area of research in the future.

4.3. Enhance flexibility

With the rapid development of e-skin and wearable devices, the flexibility of triboelectric sensors has increased. Conducting treatments on flexible materials and altering the spatial organisation of materials are the main ways to improve the flexibility of electrode materials. For example, flexible conductive hydrogel materials exhibit both conductivity and excellent flexibility. The reconstruction of the material space structure can use silk wire electrode material to fabricate fabric structure electrodes. Therefore, a crucial area of research for triboelectric sensors in the future is to increase their flexibility.

4.4. Simplify process

At present, the electrode material processing technology of triboelectric pressure sensors is limited by complex processes and high cost. Multiple procedures are frequently necessary to increase the performance of sensors, which also results in complex operations. Too many technological processes also significantly affect the production of sensors. However, although the use of high-precision machining technology can improve sensor sensitivity to a certain extent, it also increases

Fig. 11. Conclusions and perspectives of triboelectric pressure sensors.

processing complexity and costs. Simplifying the process while considering sensor performance and cost is a necessary problem. The update of material pre-treatment technology and high-precision machining technology will better balance the development requirements of simplifying the manufacturing process and improving the sensing performance in the future. Therefore, simplifying the triboelectric pressure sensor material manufacturing technology is also a key area for future studies.

CRediT authorship contribution statement

Linan Guo: Investigation, Software, Figures, Writing – review & editing. **Guitao Wu**: Tables and Writing – review & editing. **Yongjiu Zou**: Figures and Writing – review & editing. **Minyi Xu**: Conceptualization, Methodology, Writing – review & editing. **Qunyi Wang**: Visualization, References. **Tong Li**: Visualization, References. **Bohan Yao:** Visualization, References.

Declaration of Competing Interest

The authors declare that they have no known competing financial interests or personal relationships that could have appeared to influence the work reported in this paper.

Data Availability

No data was used for the research described in the article.

Acknowledgments

The authors are grateful for the support received from the National Key Research and Development Project from the Minister of Science and Technology (2021YFA1201604), the National Natural Science Foundation of China (51879022, 52101400, 52101382), and the Dalian Outstanding Young Scientific and Technological Talents Project (2021RJ11).

References

[1] L. Liu, X. Guo, W. Liu, C. Lee, Recent progress in the energy harvesting technology-from self-powered sensors to self-sustained IoT, and new applications, Nanomaterials 11 (2021) 2975, https://doi.org/10.3390/nano11112975.

[2] L. Liu, Q. Shi, Z. Sun, C. Lee, Magnetic-interaction assisted hybridized triboelectric-electromagnetic nanogenerator for advanced human-machine interfaces, Nano Energy 86 (2021), 106154, https://doi.org/10.1016/j.nanoen.2021.106154.

[3] C. Qiu, F. Wu, C. Lee, M.R. Yuce, Self-powered control interface based on Gray code with hybrid triboelectric and photovoltaics energy harvesting for IoT smart home and access control applications, Nano Energy 70 (2020), 104456, https://doi.org/10.1016/j.nanoen.2020.104456.

[4] Z. Song, W. Ye, Z. Chen, Z. Chen, M. Li, W. Tang, et al., Wireless self-powered high-performance integrated nanostructured-gas-sensor network for future smart homes, ACS Nano 15 (2021) 7659–7667, https://doi.org/10.1021/acsnano.1c01256.

[5] S. Wang, X. Wang, Z.L. Wang, Y. Yang, Efficient scavenging of solar and wind energies in a smart city, ACS Nano 10 (2016) 5696–5700, https://doi.org/10.1021/acsnano.6b02575.

[6] Z. Zhang, Q. Shi, T. He, X. Guo, B. Dong, J. Lee, et al., Artificial intelligence of toilet (AI-Toilet) for an integrated health monitoring system (IHMS) using smart triboelectric pressure sensors and image sensor, Nano Energy 90 (2021), 106517, https://doi.org/10.1016/j.nanoen.2021.106517.

[7] B.M. Eskofier, S.I. Lee, M. Baron, A. Simon, C.F. Martindale, H. Gassner, et al., An overview of smart shoes in the internet of health things: gait and mobility assessment in health promotion and disease monitoring, Appl. Sci. -Basel 7 (2017) 986, https://doi.org/10.3390/app7100986.

[8] F. Wahl, R. Zhang, M. Freund, O. Amft, Personalizing 3D-printed smart eyeglasses to augment daily life, Computer 50 (2017) 26–35, https://doi.org/10.1109/mc.2017.44.

[9] Z. Wen, M.-H. Yeh, H. Guo, J. Wang, Y. Zi, W. Xu, et al., Self-powered textile for wearable electronics by hybridizing fiber-shaped nanogenerators, solar cells, and supercapacitors, Sci. Adv. 2 (2016) 1600097, https://doi.org/10.1126/sciadv.1600097.

[10] B. Reeder, A. David, Health at hand: a systematic review of smart watch uses for health and wellness, J. Biomed. Inform. 63 (2016) 269–276, https://doi.org/10.1016/j.jbi.2016.09.001.

[11] M. Zhu, Y. Wang, M. Lou, J. Yu, Z. Li, B. Ding, Bioinspired transparent and antibacterial electronic skin for sensitive tactile sensing, Nano Energy 81 (2021), 105669, https://doi.org/10.1016/j.nanoen.2020.105669.

[12] H. Wu, Z. Su, M. Shi, L. Miao, Y. Song, H. Chen, et al., Self-powered noncontact electronic skin for motion sensing, Adv. Funct. Mater. 28 (2018) 99–108, https://doi.org/10.1002/adfm.201704641.

[13] X. Han, D. Jiang, X. Qu, Y. Bai, Y. Cao, R. Luo, et al., A stretchable, self-healable triboelectric nanogenerator as electronic skin for energy harvesting and tactile sensing, Materials 14 (2021) 1689, https://doi.org/10.3390/ma14071689.

[14] H. Guo, J. Wan, H. Wu, H. Wang, L. Miao, Y. Song, et al., Self-powered multifunctional electronic skin for a smart anti-counterfeiting signature system, ACS Appl. Mater. Interfaces 12 (2020) 22357–22364, https://doi.org/10.1021/acsami.0c03510.

[15] C. Jia, Y. Zhu, F. Sun, T. Zhao, R. Xing, Y. Mao, et al., A flexible and stretchable self-powered nanogenerator in basketball passing technology monitoring, Electronics 10 (2021) 2584, https://doi.org/10.3390/electronics10212584.

[16] Z. Lu, Y. Zhu, C. Jia, T. Zhao, M. Bian, C. Jia, et al., A self-powered portable flexible sensor of monitoring speed skating techniques, Biosensors 11 (2021) 108, https://doi.org/10.3390/bios11040108.

[17] Y. Mao, Y. Zhu, T. Zhao, C. Jia, M. Bian, X. Li, et al., A portable and flexible self-powered multifunctional sensor for real-time monitoring in swimming, Biosensors 11 (2021) 147, https://doi.org/10.3390/bios11050147.

[18] Y. Mao, F. Sun, Y. Zhu, C. Jia, T. Zhao, C. Huang, et al., Nanogenerator-based wireless intelligent motion correction system for storing mechanical energy of human motion, Sustainability 14 (2022) 6944, https://doi.org/10.3390/su14116944.

[19] F. Sun, Y. Zhu, C. Jia, B. Ouyang, T. Zhao, C. Li, et al., A flexible lightweight triboelectric nanogenerator for protector and scoring system in taekwondo competition monitoring, Electronics 11 (2022) 1306, https://doi.org/10.3390/electronics11091306.

[20] J. Xu, X. Wei, R. Li, Y. Shi, Y. Peng, Z. Wu, et al., Intelligent self-powered sensor based on triboelectric nanogenerator for take-off status monitoring in the sport of triple-jumping, Nano Res. 15 (2022) 6483–6489, https://doi.org/10.1007/s12274-022-4218-5.

[21] Y. Shao, F. Zhou, F. Wang, A triboelectric sensor with a dual working unit for race walking motion monitoring, J. Electron. Mater. 51 (2022) 3569–3578, https://doi.org/10.1007/s11664-022-09597-5.

[22] Y. Mao, Y. Zhu, T. Zhao, C. Jia, X. Wang, Q. Wang, Portable mobile gait monitor system based on triboelectric nanogenerator for monitoring gait and powering electronics, Energies 14 (2021) 4996, https://doi.org/10.3390/en14164996.

[23] S. Lim, D. Son, J. Kim, Y.B. Lee, J.-K. Song, S. Choi, et al., Transparent and stretchable interactive human machine interface based on patterned graphene heterostructures, Adv. Funct. Mater. 25 (2015) 375–383, https://doi.org/10.1002/adfm.201402987.

[24] M. Zhu, Z. Sun, Z. Zhang, Q. Shi, T. He, H. Liu, et al., Haptic-feedback smart glove as a creative human-machine interface (HMI) for virtual/augmented reality applications, Sci. Adv. 6 (2020) 19, https://doi.org/10.1126/sciadv.aaz8693.

[25] J. Lee, S. Pyo, D.-S. Kwon, E. Jo, W. Kim, J. Kim, Ultrasensitive strain sensor based on separation of overlapped carbon nanotubes, Small 15 (2019) 1805120, https://doi.org/10.1002/smll.201805120.

[26] S. Choi, K. Yoon, S. Lee, H.J. Lee, J. Lee, D.W. Kim, et al., Conductive hierarchical hairy fibers for highly sensitive, stretchable, and water-resistant multimodal gesture-distinguishable sensor, VR applications, Adv. Funct. Mater. 29 (2019) 1905808, https://doi.org/10.1002/adfm.201905808.

[27] B. Dong, Y. Yang, Q. Shi, S. Xu, Z. Sun, S. Zhu, et al., Wearable triboelectric-human-machine interface (THMI) using robust nanophotonic readout, ACS Nano 14 (2020) 8915–8930, https://doi.org/10.1021/acsnano.0c03728.

[28] P. Xu, J. Liu, X. Liu, X. Wang, J. Zheng, S. Wang, et al., A bio-inspired and self-powered triboelectric tactile sensor for underwater vehicle perception, npj Flex. Electron. 6 (2022) 25, https://doi.org/10.1038/s41528-022-00160-0.

[29] F. Peng, M. Gao, Z. Han, D. Liu, K. Dai, L. Mi, et al., One-step fabrication of sandwiched film based triboelectric nanogenerator for large-area energy harvester and precise self-powered sensor, Nano Energy 103 (2022), 107771, https://doi.org/10.1016/j.nanoen.2022.107771.

[30] P. Xu, X. Wang, S. Wang, T. Chen, J. Liu, J. Zheng, et al., A triboelectric-based artificial whisker for reactive obstacle avoidance and local mapping, Research 2021 (2021) 9864967, https://doi.org/10.34133/2021/9864967.

[31] Y. Yang, H. Zhang, Z.-H. Lin, Y.S. Zhou, Q. Jing, Y. Su, et al., Human skin based triboelectric nanogenerators for harvesting biomechanical energy and as self-powered active tactile sensor system, ACS Nano 7 (2013) 9213–9222, https://doi.org/10.1021/nn403838y.

[32] J. Zhong, H. Zhu, Q. Zhong, J. Dai, W. Li, S.-H. Jang, et al., Self-powered human-interactive transparent nanopaper systems, ACS Nano 9 (2015) 7399–7406, https://doi.org/10.1021/acsnano.5b02414.

[33] K. Dong, Z. Wu, J. Deng, A.C. Wang, H. Zou, C. Chen, et al., A stretchable yarn embedded triboelectric nanogenerator as electronic skin for biomechanical energy harvesting and multifunctional pressure sensing, Adv. Mater. 30 (2018) 1804944, https://doi.org/10.1002/adma.201804944.

[34] S.W. Chen, X. Cao, N. Wang, L. Ma, H.R. Zhu, M. Willander, et al., An ultrathin flexible single-electrode triboelectric-nanogenerator for mechanical energy harvesting and instantaneous force sensing, Adv. Energy Mater. 7 (2017) 1601255, https://doi.org/10.1002/aenm.201601255.

[35] G. Zhu, W.Q. Yang, T. Zhang, Q. Jing, J. Chen, Y.S. Zhou, et al., Self-powered, ultrasensitive, flexible tactile sensors based on contact electrification, Nano Lett. 14 (2014) 3208–3213, https://doi.org/10.1021/nl5005652.

[36] P. Xu, J. Zheng, J. Liu, X. Liu, X. Wang, S. Wang, et al., Deep learning assisted underwater 3D tactile tensegrity, Research 2023 (2023) 1–49, https://doi.org/10.34133/research.0062.
[37] J. Zhao, F. Li, Z. Wang, P. Dong, G. Xia, K. Wang, Flexible PVDF nanogenerator-driven motion sensors for human body motion energy tracking and monitoring, J. Mater. Sci. -Mater. Electron. 32 (2021) 14715–14727, https://doi.org/10.1007/s10854-021-06027-w.
[38] J. Xiong, J. Chen, P.S. Lee, Functional fibers and fabrics for soft robotics, wearables, and human-robot interface, Adv. Mater. 33 (2021) 2002640, https://doi.org/10.1002/adma.202002640.
[39] C. Wang, L. Dong, D. Peng, C. Pan, Tactile sensors for advanced intelligent systems, Adv. Intell. Syst. 1 (2019) 1900090, https://doi.org/10.1002/aisy.201900090.
[40] J. Timana, C. Montufar, R. Ccorahua, E.A. Vela, Self-powered triboelectric nanosensors for soft endoscopic and catheter applications, Int. Conf. Manip., Autom. Robot. Small Scales (MARSS) (2020) 65–66, https://doi.org/10.1109/MARSS49294.2020.9307923.
[41] Y.-C. Lai, J. Deng, R. Liu, Y.-C. Hsiao, S.L. Zhang, W. Peng, et al., Actively perceiving and responsive soft robots enabled by self-powered, highly extensible, and highly sensitive triboelectric proximity- and pressure-sensing skins, Adv. Mater. 30 (2018) 1801114, https://doi.org/10.1002/adma.201801114.
[42] M. Ha, S. Lim, S. Cho, Y. Lee, S. Na, C. Baig, et al., Skin-inspired hierarchical polymer architectures with gradient stiffness for spacer-free, ultrathin, and highly sensitive triboelectric sensors, ACS Nano 12 (2018) 3964–3974, https://doi.org/10.1021/acsnano.8b01557.
[43] X. Li, C. Xu, C. Wang, J. Shao, X. Chen, C. Wang, et al., Improved triboelectrification effect by bendable and slidable fish-scale-like microstructures, Nano Energy 40 (2017) 646–654, https://doi.org/10.1016/j.nanoen.2017.09.013.
[44] G. Zhao, Y. Zhang, N. Shi, Z. Liu, X. Zhang, M. Wu, et al., Transparent and stretchable triboelectric nanogenerator for self-powered tactile sensing, Nano Energy 59 (2019) 302–310, https://doi.org/10.1016/j.nanoen.2019.02.054.
[45] M. Wu, Z. Gao, K. Yao, S. Hou, Y. Liu, D. Li, et al., Thin, soft, skin-integrated foam-based triboelectric nanogenerators for tactile sensing and energy harvesting, Mater. Today Energy 20 (2021), 100657, https://doi.org/10.1016/j.mtener.2021.100657.
[46] Y. Zhao, W. Gao, K. Dai, S. Wang, Z. Yuan, J. Li, et al., Bioinspired multifunctional photonic-electronic smart skin for ultrasensitive health monitoring, for visual and self-powered sensing, Adv. Mater. 33 (2021) 2102332, https://doi.org/10.1002/adma.202102332.
[47] G. Yao, L. Xu, X. Cheng, Y. Li, X. Huang, W. Guo, et al., Bioinspired triboelectric nanogenerators as self-powered electronic skin for robotic tactile sensing, Adv. Funct. Mater. 30 (2020) 1907312, https://doi.org/10.1002/adfm.201907312.
[48] M. Peng, Z. Wen, L. Xie, J. Cheng, Z. Jia, D. Shi, et al., 3D printing of ultralight biomimetic hierarchical graphene materials with exceptional stiffness and resilience, Adv. Mater. 31 (2019) 1902930, https://doi.org/10.1002/adma.201902930.
[49] F.-R. Fan, L. Lin, G. Zhu, W. Wu, R. Zhang, Z.L. Wang, Transparent triboelectric nanogenerators and self-powered pressure sensors based on micropatterned plastic films, Nano Lett. 12 (2012) 3109–3114, https://doi.org/10.1021/nl300988z.
[50] M.-L. Seol, J.-H. Woo, D.-I. Lee, H. Im, J. Hur, Y.-K. Choi, Nature-replicated nano-in-micro structures for triboelectric energy harvesting, Small 10 (2014) 3887–3894, https://doi.org/10.1002/smll.201400863.
[51] Q. Zhou, J.G. Park, K.N. Kim, A.K. Thokchom, J. Bae, J.M. Baik, et al., Transparent-flexible-multimodal triboelectric nanogenerators for mechanical energy harvesting and self-powered sensor applications, Nano Energy 48 (2018) 471–480, https://doi.org/10.1016/j.nanoen.2018.03.074.
[52] X.-F. Zhao, C.-Z. Hang, X.-H. Wen, M.-Y. Liu, H. Zhang, F. Yang, et al., Ultrahigh-sensitive finlike double-sided e-skin for force direction detection, ACS Appl. Mater. Interfaces 12 (2020) 14136–14144, https://doi.org/10.1021/acsami.9b23110.
[53] Z. Yang, Y. Pang, Y. X.-l. Han, J. Yang, M. Ling, Jian, et al., Graphene textile strain sensor with negative resistance variation for human motion detection, ACS Nano 12 (2018) 9134–9141, https://doi.org/10.1021/acsnano.8b03391.
[54] Y. Gao, C. Yan, H. Huang, T. Yang, G. Tian, D. Xiong, et al., Microchannel-confined MXene based flexible piezoresistive multifunctional micro-force sensor, Adv. Funct. Mater. 30 (2020) 1909603, https://doi.org/10.1002/adfm.201909603.
[55] J. Zhao, C. He, R. Yang, Z. Shi, M. Cheng, W. Yang, et al., Ultra-sensitive strain sensors based on piezoresistive nanographene films, Appl. Phys. Lett. 101 (2012), 063112, https://doi.org/10.1063/1.4742331.
[56] J. Shi, L. Wang, Z. Dai, L. Zhao, M. Du, H. Li, et al., Multiscale hierarchical design of a flexible piezoresistive pressure sensor with high sensitivity and wide linearity range, Small 14 (2018) 1800819, https://doi.org/10.1002/smll.201800819.
[57] Y. Wan, Z. Qiu, J. Huang, J. Yang, Q. Wang, P. Lu, et al., Natural plant materials as dielectric layer for highly sensitive flexible electronic skin, Small 14 (2018) 1801657, https://doi.org/10.1002/smll.201801657.
[58] S. Chen, L. Sun, X. Zhou, Y. Guo, J. Song, S. Qian, et al., Mechanically and biologically skin-like elastomers for bio-integrated electronics, Nat. Commun. 11 (2020) 1107, https://doi.org/10.1038/s41467-020-14446-2.
[59] Y. Xiong, Y. Shen, L. Tian, Y. Hu, P. Zhu, R. Sun, et al., A flexible, ultra-highly sensitive and stable capacitive pressure sensor with convex microarrays for motion and health monitoring, Nano Energy 70 (2020), 104436, https://doi.org/10.1016/j.nanoen.2019.104436.
[60] J. Zhang, L. Wan, Y. Gao, X. Fang, T. Lu, L. Pan, et al., Highly stretchable and self-healable MXene/polyvinyl alcohol hydrogel electrode for wearable capacitive electronic skin, Adv. Electron. Mater. 5 (2019) 1900285, https://doi.org/10.1002/aelm.201900285.
[61] W. Hu, X. Niu, R. Zhao, Q. Pei, Elastomeric transparent capacitive sensors based on an interpenetrating composite of silver nanowires and polyurethane, Appl. Phys. Lett. 102 (2013), 083303, https://doi.org/10.1063/1.4794143.
[62] X. Li, Y. Wang, S. Sun, T. He, Q. Hu, Y. Yang, et al., Flexible and ultrasensitive piezoelectric composites based on highly (00l)-assembled BaTio3 microplatelets for wearable electronics application, Adv. Mater. Technol. 4 (2019) 1900689, https://doi.org/10.1002/admt.201900689.
[63] M. Zhu, M. Lou, I. Abdalla, J. Yu, Z. Li, B. Ding, Highly shape adaptive fiber based electronic skin for sensitive joint motion monitoring and tactile sensing, Nano Energy 69 (2020), 104429, https://doi.org/10.1016/j.nanoen.2019.104429.
[64] Y. Yang, H. Pan, G. Xie, Y. Jiang, C. Chen, Y. Su, et al., Flexible piezoelectric pressure sensor based on polydopamine-modified BaTiO3/PVDF composite film for human motion monitoring, Sens. Actuators a-Phys. 301 (2020), 111789, https://doi.org/10.1016/j.sna.2019.111789.
[65] J. Luo, L. Zhang, T. Wu, H. Song, C. Tang, Flexible piezoelectric pressure sensor with high sensitivity for electronic skin using near-field electrohydrodynamic direct-writing method, Extrem. Mech. Lett. 48 (2021), 101279, https://doi.org/10.1016/j.eml.2021.101279.
[66] A.A. Kazaryan, A thin-film piezoelectric pressure sensor, Meas. Tech. 45 (2002) 515–518, https://doi.org/10.1023/a:1020068006447.
[67] X. Hou, S. Zhang, J. Yu, M. Cui, J. He, L. Li, et al., Flexible piezoelectric nanofibers/polydimethylsiloxane-based pressure sensor for self-powered human motion monitoring, Energy Technol. 8 (2020) 1901242, https://doi.org/10.1002/ente.201901242.
[68] Z. Chen, Z. Wang, X. Li, Y. Lin, N. Luo, M. Long, et al., Flexible piezoelectric-induced pressure sensors for static measurements based on nanowires/graphene heterostructures, ACS Nano 11 (2017) 4507–4513, https://doi.org/10.1021/acsnano.6b08027.
[69] Y. Ma, N. Liu, L. Li, X. Hu, Z. Zou, J. Wang, et al., A highly flexible and sensitive piezoresistive sensor based on MXene with greatly changed interlayer distances, Nat. Commun. 8 (2017) 1207, https://doi.org/10.1038/s41467-017-01136-9.
[70] J. Yang, J. An, Y. Sun, J. Zhang, L. Zu, H. Li, et al., Transparent self-powered triboelectric sensor based on PVA/PA hydrogel for promoting human-machine interaction in nursing and patient safety, Nano Energy 97 (2022), 107199, https://doi.org/10.1016/j.nanoen.2022.107199.
[71] M. Habib, I. Lantgios, K. Hornbostel, A review of ceramic, polymer and composite piezoelectric materials, J. Phys. D. -Appl. Phys. 55 (2022), 423002, https://doi.org/10.1088/1361-6463/ac8687.
[72] X. Li, M. Sun, X. Wei, C. Shan, Q. Chen, 1D piezoelectric material based nanogenerators: methods, materials and property optimization, Nanomaterials 8 (2018) 188, https://doi.org/10.3390/nano8040188.
[73] X.-Q. Fang, J.-X. Liu, V. Gupta, Fundamental formulations and recent achievements in piezoelectric Chemical Engineering Journal.
[74] C. Chen, X. Wang, Y. Wang, D. Yang, F. Yao, W. Zhang, et al., Additive manufacturing of piezoelectric materials, Adv. Funct. Mater. 30 (2020) 2005141, https://doi.org/10.1002/adfm.202005141.
[75] R. Xu, F. Luo, Z. Zhu, M. Li, B. Chen, Flexible wide-range triboelectric sensor for physiological signal monitoring and human motion recognition, ACS Appl. Electron. Mater. (2022))4151–)4160, https://doi.org/10.1021/acsaelm.2c00681.
[76] S.R.A. Ruth, V.R. Feig, H. Tran, Z. Bao, Microengineering pressure sensor active layers for improved performance, Adv. Funct. Mater. 30 (2020) 2003491, https://doi.org/10.1002/adfm.202003491.
[77] M.S. Rasel, H.O. Cho, J.W. Kim, J.Y. Park, Iop, A self-powered triboelectric sensor for wide-range pressure detection in wearable application, 17th International Conference on Micro and Nanotechnology for Power Generation and Energy Conversion Applications (PowerMEMS), 1052(2017)012029.https://doi.org/10.1088/1742–6596/1052/1/012029.
[78] K. Parida, V. Bhavanasi, V. Kumar, R. Bendi, P.S. Lee, Self-powered pressure sensor for ultra-wide range pressure detection, Nano Res. 10 (2017) 3557–3570, https://doi.org/10.1007/s12274-017-1567-6.
[79] P.S. Das, A. Chhetry, P. Maharjan, M.S. Rasel, J.Y. Park, A laser ablated graphene-based flexible self-powered pressure sensor for human gestures and finger pulse monitoring, Nano Res. 12 (2019) 1789–1795, https://doi.org/10.1007/s12274-019-2433-5.
[80] Y. Chen, D. Li, Y. Xu, Z. Ling, H. Nawaz, S. Chen, et al., Surface-microstructured cellulose films toward sensitive pressure sensors and efficient triboelectric nanogenerators, Int. J. Biol. Macromol. 208 (2022) 324–332, https://doi.org/10.1016/j.ijbiomac.2022.03.123.
[81] S. Kim, M. Amjadi, T.-l. Lee, Y. Jeon, D. Kwon, M.S. Kim, et al., WIDE RANGE-SENSITIVE, BENDING-INSENSITIVE PRESSURE DETECTION AND APPLICATION TO WEARABLE HEALTHCARE DEVICE, 20th International Conference on Solid-State Sensors, Actuators and Microsystems and Eurosensors XXXIII (TRANSDUCERS and EUROSENSORS), (2019) 374–377. https://doi.org/10.1109/TRANSDUCERS.2019.8808529.
[82] S. Chatterjee, S. Saha, S.R. Barman, I. Khan, Y.-P. Pao, S. Lee, et al., Enhanced sensing performance of triboelectric nanosensors by solid-liquid contact electrification, Nano Energy 77 (2020), 105093, https://doi.org/10.1016/j.nanoen.2020.105093.
[83] S.L. Zhang, Y.-C. Lai, X. He, R. Liu, Y. Zi, Z.L. Wang, Auxetic foam-based contact-mode triboelectric nanogenerator with highly sensitive self-powered strain

sensing capabilities to monitor human body movement, Adv. Funct. Mater. 27 (2017) 1606695, https://doi.org/10.1002/adfm.201606695.
[84] X. Wang, H. Zhang, L. Dong, X. Han, W. Du, J. Zhai, et al., Self-powered high-resolution and pressure-sensitive triboelectric sensor matrix for real-time tactile mapping, Adv. Mater. 28 (2016) 2896–2903, https://doi.org/10.1002/adma.201503407.
[85] M.S. Rasel, P. Maharjan, M. Salauddin, M.T. Rahman, H.O. Cho, J.W. Kim, et al., An impedance tunable and highly efficient triboelectric nanogenerator for large-scale, ultra-sensitive pressure sensing applications, Nano Energy 49 (2018) 603–613, https://doi.org/10.1016/j.nanoen.2018.04.060.
[86] C. Lin, J. Lan, J. Yu, Z. Hua, H. Huang, X. Ma, et al., Cocklebur-structured design of plant fibers for high-performance triboelectric nanogenerators and pressure sensors, Mater. Today Commun. 30 (2022), 103208, https://doi.org/10.1016/j.mtcomm.2022.103208.
[87] H. Lei, K. Cao, Y. Chen, Z. Liang, Z. Wen, L. Jiang, et al., 3D-printed endoplasmic reticulum rGO microstructure based self-powered triboelectric pressure sensor, Chem. Eng. J. 445 (2022), 136821, https://doi.org/10.1016/j.cej.2022.136821.
[88] H.J. Lee, K.-Y. Chun, J.H. Oh, C.-S. Han, Wearable triboelectric strain-insensitive pressure sensors based on hierarchical superposition patterns, ACS Sens. 6 (2021) 2411–2418, https://doi.org/10.1021/acssensors.1c00640.
[89] H. Kou, H. Wang, R. Cheng, Y. Liao, X. Shi, J. Luo, et al., Smart pillow based on flexible and breathable triboelectric nanogenerator arrays for head movement monitoring during sleep, ACS Appl. Mater. Interfaces 14 (2022) 23998–24007, https://doi.org/10.1021/acsami.2c03056.
[90] C. Jeong, S. Lee, H.D. Roh, M.Q. Feng, Y.-B. Park, Hierarchically structured ZnO nanorod-carbon fiber composites as ultrathin, flexible, highly sensitive triboelectric sensors, Smart Mater. Struct. 29 (2020), 025002, https://doi.org/10.1088/1361-665X/ab5b5f.
[91] H. Zhao, M. Xu, M. Shu, J. An, W. Ding, X. Liu, et al., Underwater wireless communication via TENG-generated Maxwell's displacement current, Nat. Commun. 13 (2022) 3325, https://doi.org/10.1038/s41467-022-31042-8.
[92] T. Zhao, M. Xu, X. Xiao, Y. Ma, Z. Li, Z.L. Wang, Recent progress in blue energy harvesting for powering distributed sensors in ocean, Nano Energy 88 (2021), 106199, https://doi.org/10.1016/j.nanoen.2021.106199.
[93] Z. Xu, C. Wu, F. Li, W. Chen, T. Guo, T.W. Kim, Triboelectric electronic-skin based on graphene quantum dots for application in self-powered, smart, artificial fingers, Nano Energy 49 (2018) 274–282, https://doi.org/10.1016/j.nanoen.2018.04.059.
[94] J. Rao, Z. Chen, D. Zhao, R. Ma, W. Yi, C. Zhang, et al., Tactile electronic skin to simultaneously detect and distinguish between temperature and pressure based on a triboelectric nanogenerator, Nano Energy 75 (2020), 105073, https://doi.org/10.1016/j.nanoen.2020.105073.
[95] X. Peng, K. Dong, C. Ye, Y. Jiang, S. Zhai, R. Cheng, et al., A breathable, biodegradable, antibacterial, and self-powered electronic skin based on all-nanofiber triboelectric nanogenerators, Sci. Adv. 6 (2020) 26, https://doi.org/10.1126/sciadv.aba9624.
[96] J. Park, D. Kim, Y.T. Kim, Soft and transparent triboelectric nanogenerator based E-skin for wearable energy harvesting and pressure sensing, Nanotechnology 32 (2021) 38, https://doi.org/10.1088/1361-6528/ac0c3f.
[97] Y. Fu, H. He, Y. Liu, Q. Wang, L. Xing, X. Xue, Self-powered, stretchable, fiber-based electronic-skin for actively detecting human motion and environmental atmosphere based on a triboelectrification/gas-sensing coupling effect, J. Mater. Chem. C. 5 (2017) 1231–1239, https://doi.org/10.1039/c6tc04272d.
[98] Y.-W. Cai, G.-G. Wang, Y.-C. Mei, D.-Q. Zhao, J.-J. Peng, N. Sun, et al., Self-healable, super-stretchable and shape-adaptive triboelectric nanogenerator based on double cross-linked PDMS for electronic skins, Nano Energy 102 (2022), 107683, https://doi.org/10.1016/j.nanoen.2022.107683.
[99] Z. Xu, D. Zhang, H. Cai, Y. Yang, H. Zhang, C. Du, Performance enhancement of triboelectric nanogenerators using contact-separation mode in conjunction with the sliding mode and multifunctional application for motion monitoring, Nano Energy 102 (2022), 107719, https://doi.org/10.1016/j.nanoen.2022.107719.
[100] H. Lei, Y. Chen, Z. Gao, Z. Wen, X. Sun, Advances in self-powered triboelectric pressure sensors, J. Mater. Chem. A 9 (2021) 20100–20130, https://doi.org/10.1039/d1ta03505c.
[101] U. Pierre Claver, G. Zhao, Recent progress in flexible pressure sensors based electronic skin, Adv. Eng. Mater. 23 (2021) 2001187, https://doi.org/10.1002/adem.202001187.
[102] Y. Zou, V. Raveendran, J. Chen, Wearable triboelectric nanogenerators for biomechanical energy harvesting, Nano Energy 77 (2020), 105303, https://doi.org/10.1016/j.nanoen.2020.105303.
[103] Y. Zou, J. Xu, K. Chen, J. Chen, Advances in nanostructures for high-performance triboelectric nanogenerators, Adv. Mater. Technol. 6 (2021) 2000916, https://doi.org/10.1002/admt.202000916.
[104] K. Tao, Z. Chen, H. Yi, R. Zhang, Q. Shen, J. Wu, et al., Hierarchical honeycomb-structured electret/triboelectric nanogenerator for biomechanical and morphing wing energy harvesting, Nano-Micro Lett. 13 (2021), https://doi.org/10.1007/s40820-021-00644-0.
[105] L. Yao, H. Zhang, J. Jiang, Z. Zhang, X. Zheng, Recent progress in sensing technology based on triboelectric nanogenerators in dynamic behaviors, Sensors 22 (2022) 123, https://doi.org/10.3390/s22134837.
[106] J. Tao, R. Bao, X. Wang, Y. Peng, J. Li, S. Fu, et al., Self-powered tactile sensor array systems based on the triboelectric effect, Adv. Funct. Mater. 29 (2019) 1806379, https://doi.org/10.1002/adfm.201806379.
[107] X. Pu, S. An, Q. Tang, H. Guo, C. Hu, Wearable triboelectric sensors for biomedical monitoring and human-machine interface, Iscience 24 (2021), 102027, https://doi.org/10.1016/j.isci.2020.102027.
[108] H. Pan, T.-W. Lee, Recent progress in development of wearable pressure sensors derived from biological materials, Adv. Healthc. Mater. 10 (2021) 2100460, https://doi.org/10.1002/adhm.202100460.
[109] C. Bu, F. Li, K. Yin, J. Pang, L. Wang, K. Wang, Research progress and prospect of triboelectric nanogenerators as self-powered human body sensors, Acs Appl. Electron. Mater. 2 (2020) 863–878, https://doi.org/10.1021/acsaelm.0c00022.
[110] P. Zhang, Z. Zhang, J. Cai, A foot pressure sensor based on triboelectric nanogenerator for human motion monitoring, Microsyst. Technol. -Micro-Nanosyst. -Inf. Storage Process. Syst. 27 (2021) 3507–3512, https://doi.org/10.1007/s00542-020-05199-5.
[111] M. Zhang, Y. Jie, X. Cao, J. Bian, T. Li, N. Wang, et al., Robust design of unearthed single-electrode TENG from three-dimensionally hybridized copper/polydimethylsiloxane film, Nano Energy 30 (2016) 155–161, https://doi.org/10.1016/j.nanoen.2016.10.002.
[112] J. Yu, X. Hou, M. Cui, S. Shi, J. He, Y. Sun, et al., Flexible PDMS-based triboelectric nanogenerator for instantaneous force sensing and human joint movement monitoring, Sci. China-Mater. 62 (2019) 1423–1432, https://doi.org/10.1007/s40843-019-9446-1.
[113] X. Shen, W. Han, Y. Jiang, Q. Ding, X. Li, X. Zhao, et al., Punching pores on cellulose fiber paper as the spacer of triboelectric nanogenerator for monitoring human motion, Energy Rep. 6 (2020) 2851–2860, https://doi.org/10.1016/j.egyr.2020.10.011.
[114] Z. Ding, M. Zou, P. Yao, L. Fan, A triboelectric nanogenerator for mechanical energy harvesting and as self-powered pressure sensor, Microelectron. Eng. 257 (2022), 111725, https://doi.org/10.1016/j.mee.2022.111725.
[115] Z. Dai, N. Wang, Y. Yu, Y. Lu, L. Jiang, D.-A. Zhang, et al., One-step preparation of a core-spun Cu/P(VDF-TrFE) nanofibrous yarn for wearable smart textile to monitor human movement, ACS Appl. Mater. Interfaces 13 (2021) 44234–44242, https://doi.org/10.1021/acsami.1c10366.
[116] D. Wang, D. Zhang, J. Guo, Y. Hu, Y. Yang, T. Sun, et al., Multifunctional poly (vinyl alcohol)/Ag nanofibers-based triboelectric nanogenerator for self-powered MXene/tungsten oxide nanohybrid NO2 gas sensor, Nano Energy 89 (2021), 106410, https://doi.org/10.1016/j.nanoen.2021.106410.
[117] D. Wang, D. Zhang, Y. Yang, Q. Mi, J. Zhang, L. Yu, Multifunctional latex/polytetrafluoroethylene-based triboelectric nanogenerator for self-powered organ-like mxene/metal-organic framework-derived cuo nanohybrid ammonia sensor, ACS Nano 15 (2021) 2911–2919, https://doi.org/10.1021/acsnano.0c09015.
[118] K. Tao, H. Yi, Y. Yang, H. Chang, J. Wu, L. Tang, et al., Origami-inspired electret-based triboelectric generator for biomechanical and ocean wave energy harvesting, Nano Energy 67 (2020), 104197, https://doi.org/10.1016/j.nanoen.2019.104197.
[119] A. You, X. Zhang, X. Peng, K. Dong, Y. Lu, Q. Zhang, A skin-inspired triboelectric nanogenerator with an interpenetrating structure for motion sensing and energy harvesting, Macromol. Mater. Eng. 306 (2021) 2100147, https://doi.org/10.1002/mame.202100147.
[120] T. Xiao, Y. Gao, G. Yu, M. Qian, J. Tan, F. Xuan, Wearable pressure sensor using UV-patternable silver nanowire/polydimethylsiloxane composite, Mater. Res. Express 6 (2019), 095087, https://doi.org/10.1088/2053-1591/ab31df.
[121] X. Wang, Y. Zhang, X. Zhang, Z. Huo, X. Li, M. Que, et al., A highly stretchable transparent self-powered triboelectric tactile sensor with metallized nanofibers for wearable electronics, Adv. Mater. 30 (2018) 1706738, https://doi.org/10.1002/adma.201706738.
[122] Y. Shi, X. Wei, K. Wang, D. He, Z. Yuan, J. Xu, et al., Integrated all-fiber electronic skin toward self-powered sensing sports systems, ACS Appl. Mater. Interfaces 13 (2021) 50329–50337, https://doi.org/10.1021/acsami.1c13420.
[123] V.V. Sharma, K.N. Kim, G.H. Han, E.-J. Gwak, J.-H. Woo, S.B. Kang, et al., 3D multiscale gradient pores impregnated with Ag nanowires for simultaneous pressure and bending detection with enhanced linear sensitivity, Adv. Mater. Technol. 5 (2020) 1901041, https://doi.org/10.1002/admt.201901041.
[124] D. Wang, D. Zhang, M. Tang, H. Zhang, F. Chen, T. Wang, et al., Rotating triboelectric-electromagnetic nanogenerator driven by tires for self-powered MXene-based flexible wearable electronics, Chem. Eng. J. 446 (2022), 136914, https://doi.org/10.1016/j.cej.2022.136914.
[125] X. Yu, J. Pan, J. Zhang, H. Sun, S. He, L. Qiu, et al., A coaxial triboelectric nanogenerator fiber for energy harvesting and sensing under deformation, J. Mater. Chem. A 5 (2017) 6032–6037, https://doi.org/10.1039/c7ta00248c.
[126] M. Matsunaga, J. Hirotani, S. Kishimoto, Y. Ohno, High-output, transparent, stretchable triboelectric nanogenerator based on carbon nanotube thin film toward wearable energy harvesters, Nano Energy 67 (2020), 104297, https://doi.org/10.1016/j.nanoen.2019.104297.
[127] S.A. Khan, H.L. Zhang, Y. Xie, M. Gao, M.A. Shah, A. Qadir, et al., Flexible triboelectric nanogenerator based on carbon nanotubes for self-powered weighing, Adv. Eng. Mater. 19 (2017) 1600710, https://doi.org/10.1002/adem.201600710.
[128] H. Chen, Y. Xu, L. Bai, Y. Jiang, J. Zhang, C. Zhao, et al., Crumpled graphene triboelectric nanogenerators: smaller devices with higher output performance, Adv. Mater. Technol. 2 (2017) 1700044, https://doi.org/10.1002/admt.201700044.
[129] M. Sahoo, S.-N. Lai, J.-M. Wu, M.-C. Wu, C.-S. Lai, Flexible layered-graphene charge modulation for highly stable triboelectric nanogenerator, Nanomaterials 11 (2021) 2276, https://doi.org/10.3390/nano11092276.
[130] Y.K. Fuh, S.C. Li, C.Y. Chen, C.Y. Tsai, A fully packaged self-powered sensor based on near-field electrospun arrays of poly(vinylidene fluoride) nano/micro fibers, Express Polym. Lett. 12 (2018) 136–145, https://doi.org/10.3144/expresspolymlett.2018.12.

[131] C. Jiang, X. Li, Y. Yao, L. Lan, Y. Shao, F. Zhao, et al., A multifunctional and highly flexible triboelectric nanogenerator based on MXene-enabled porous film integrated with laser-induced graphene electrode, Nano Energy 66 (2019), 104121, https://doi.org/10.1016/j.nanoen.2019.104121.
[132] P. Zhao, G. Bhattacharya, S.J. Fishlock, J.G.M. Guy, A. Kumar, C. Tsonos, et al., Replacing the metal electrodes in triboelectric nanogenerators: high-performance laser-induced graphene electrodes, Nano Energy 75 (2020), 104958, https://doi.org/10.1016/j.nanoen.2020.104958.
[133] Z. Yan, L. Wang, Y. Xia, R. Qiu, W. Liu, M. Wu, et al., Flexible high-resolution triboelectric sensor array based on patterned laser-induced graphene for self-powered real-time tactile sensing, Adv. Funct. Mater. 31 (2021) 2100709, https://doi.org/10.1002/adfm.202100709.
[134] Y. Wu, Y. Luo, J. Qu, W.A. Daoud, T. Qi, Liquid single-electrode triboelectric nanogenerator based on graphene oxide dispersion for wearable electronics, Nano Energy 64 (2019), 103948, https://doi.org/10.1016/j.nanoen.2019.103948.
[135] E. He, Y. Sun, X. Wang, H. Chen, B. Sun, B. Gu, et al., 3D angle-interlock woven structural wearable triboelectric nanogenerator fabricated with silicone rubber coated graphene oxide/cotton composite yarn, Compos. Part B-Eng. 200 (2020), 108244, https://doi.org/10.1016/j.compositesb.2020.108244.
[136] R. Wu, L. Ma, A. Patil, Z. Meng, S. Liu, C. Hou, et al., Graphene decorated carbonized cellulose fabric for physiological signal monitoring and energy harvesting, J. Mater. Chem. A 8 (2020) 12665–12673, https://doi.org/10.1039/d0ta02221g.
[137] Y. Cheng, D. Wu, S. Hao, Y. Jie, X. Cao, N. Wang, et al., Highly stretchable triboelectric tactile sensor for electronic skin, Nano Energy 64 (2019), 103907, https://doi.org/10.1016/j.nanoen.2019.103907.
[138] J. Wang, P. Cui, J. Zhang, Y. Ge, X. Liu, N. Xuan, et al., A stretchable self-powered triboelectric tactile sensor with EGaIn alloy electrode for ultra-low-pressure detection, Nano Energy 89 (2021), 106320, https://doi.org/10.1016/j.nanoen.2021.106320.
[139] J. Yi, K. Dong, S. Shen, Y. Jiang, X. Peng, C. Ye, et al., Fully fabric-based triboelectric nanogenerators as self-powered human-machine interactive keyboards, Nano-Micro Lett. 13 (2021) 103, https://doi.org/10.1007/s40820-021-00621-7.
[140] D. Wang, D. Zhang, X. Chen, H. Zhang, M. Tang, J. Wang, Multifunctional respiration-driven triboelectric nanogenerator for self-powered detection of formaldehyde in exhaled gas and respiratory behavior, Nano Energy 102 (2022), https://doi.org/10.1016/j.nanoen.2022.107711.
[141] Y. Yu, Y. Feng, F. Liu, H. Wang, H. Yu, K. Dai, et al., Carbon dots-based ultrastretchable and conductive hydrogels for high-performance tactile sensors and self-powered electronic skin, Small (2022) 2204365, https://doi.org/10.1002/smll.202204365.
[142] J. Yu, Z. Chen, H. Zeng, B. Ji, Z. Wu, J. Wu, et al., Ultra-flexible and highly transparent hydrogel-based triboelectric nanogenerator for physiological signal monitoring, 16th IEEE International Conference on Nano/Micro Engineered and Molecular Systems (IEEE-NEMS), (2021) 1903–1907. https://doi.org/10.1109/NEMS51815.2021.9451511.
[143] L. Wang, Y. Wang, S. Yang, X. Tao, Y. Zi, W.A. Daoud, Solvent-free adhesive ionic elastomer for multifunctional stretchable electronics, Nano Energy 91 (2022), 106611, https://doi.org/10.1016/j.nanoen.2021.106611.
[144] Y. Liu, T.H. Wong, X. Huang, C.K. Yiu, Y. Gao, L. Zhao, et al., Skin-integrated, stretchable, transparent triboelectric nanogenerators based on ion-conducting hydrogel for energy harvesting and tactile sensing, Nano Energy 99 (2022), 107442, https://doi.org/10.1016/j.nanoen.2022.107442.
[145] Y. Lee, S.H. Cha, Y.-W. Kim, D. Choi, J.-Y. Sun, Transparent and attachable ionic communicators based on self-cleanable triboelectric nanogenerators, Nat. Commun. 9 (2018) 1804, https://doi.org/10.1038/s41467-018-03954-x.
[146] K. Tao, Z. Chen, J. Yu, H. Zeng, J. Wu, Z. Wu, et al., Ultra-sensitive, deformable, and transparent triboelectric tactile sensor based on micro-pyramid patterned ionic hydrogel for interactive human-machine interfaces, Adv. Sci. 9 (2022) 2104168, https://doi.org/10.1002/advs.202104168.
[147] L. Lin, Y. Xie, S. Wang, W. Wu, S. Niu, X. Wen, et al., Triboelectric active sensor array for self-powered static and dynamic pressure detection and tactile imaging, ACS Nano 7 (2013) 8266–8274, https://doi.org/10.1021/nn4037514.
[148] P. Bai, G. Zhu, Q. Jing, J. Yang, J. Chen, Y. Su, et al., Membrane-based self-powered triboelectric sensors for pressure change detection and its uses in security surveillance and healthcare monitoring, Adv. Funct. Mater. 24 (2014) 5807–5813, https://doi.org/10.1002/adfm.201401267.
[149] W. Yang, J. Chen, X. Wen, Q. Jing, J. Yang, Y. Su, et al., Triboelectrification based motion sensor for human-machine interfacing, ACS Appl. Mater. Interfaces 6 (2014) 7479–7484, https://doi.org/10.1021/am500864t.
[150] X. Huo, A self-powered triboelectric pressure sensor for basketball training monitoring, Mater. Lett. 320 (2022), 132339, https://doi.org/10.1016/j.matlet.2022.132339.
[151] Y. Wu, Y. Luo, J. Qu, W.A. Daoud, T. Qi, Nanogap and environmentally stable triboelectric nanogenerators based on surface self-modified sustainable films, ACS Appl. Mater. Interfaces 12 (2020) 55444–55452, https://doi.org/10.1021/acsami.0c16671.
[152] Y. Peng, S. Xiao, J. Yang, J. Lin, W. Yuan, W. Gu, et al., The elastic microstructures of inkjet printed polydimethylsiloxane as the patterned dielectric layer for pressure sensors, Appl. Phys. Lett. 110 (2017), 261904, https://doi.org/10.1063/1.4990528.
[153] J. Jiang, Q. Guan, Y. Liu, X. Sun, Z. Wen, Abrasion and fracture self-healable triboelectric nanogenerator with ultrahigh stretchability and long-term durability, Adv. Funct. Mater. 31 (2021) 2105380, https://doi.org/10.1002/adfm.202105380.
[154] Y. Gao, L. Yu, J.C. Yeo, C.T. Lim, Flexible hybrid sensors for health monitoring: materials and mechanisms to render wearability, Adv. Mater. 32 (2020) 1902133, https://doi.org/10.1002/adma.201902133.
[155] A. Babu, I. Aazem, R. Walden, S. Bairagi, D.M. Mulvihill, S.C. Pillai, Electrospun nanofiber based TENGs for wearable electronics and self-powered sensing, Chem. Eng. J. 452 (2023), 139060, https://doi.org/10.1016/j.cej.2022.139060.
[156] S. Zhu, Y. Xia, Y. Zhu, M. Wu, C. Jia, X. Wang, High-performance triboelectric nanogenerator powered flexible electroluminescence devices based on patterned laser-induced copper electrodes for visualized information interaction, Nano Energy 96 (2022), 107116, https://doi.org/10.1016/j.nanoen.2022.107116.
[157] J. Xu, Y. Zou, A. Nashalian, J. Chen, Leverage surface chemistry for high-performance triboelectric nanogenerators, Front. Chem. 8 (2020), 577327, https://doi.org/10.3389/fchem.2020.577327.
[158] R. Liu, K. Xu, Y. Zhang, Nanomaterial-based wearable pressure sensors: a minireview, Instrum. Sci. Technol. 48 (2020) 459–479, https://doi.org/10.1080/10739149.2020.1737935.
[159] Z.L. Wang, On the first principle theory of nanogenerators from Maxwell's equations, Nano Energy 68 (2020), 104272, https://doi.org/10.1016/j.nanoen.2019.104272.
[160] Z.L. Wang, On the expanded Maxwell's equations for moving charged media system-General theory, mathematical solutions and applications in TENG, Mater. Today 52 (2022) 348–363, https://doi.org/10.1016/j.mattod.2021.10.027.
[161] Z.L. Wang, On Maxwell's displacement current for energy and sensors: the origin of nanogenerators, Mater. Today 20 (2017) 74–82, https://doi.org/10.1016/j.mattod.2016.12.001.
[162] Z.L. Wang, T. Jiang, L. Xu, Toward the blue energy dream by triboelectric nanogenerator networks, Nano Energy 39 (2017) 9–23, https://doi.org/10.1016/j.nanoen.2017.06.035.
[163] W. Song, B. Gan, T. Jiang, Y. Zhang, A. Yu, H. Yuan, et al., Nanopillar arrayed triboelectric nanogenerator as a self-powered sensitive sensor for a sleep monitoring system, ACS Nano 10 (2016) 8097–8103, https://doi.org/10.1021/acsnano.6b04344.
[164] Q. Zheng, B. Shi, F. Fan, X. Wang, L. Yan, W. Yuan, et al., In vivo powering of pacemaker by breathing-driven implanted triboelectric nanogenerator, Adv. Mater. 26 (2014) 5851–5856, https://doi.org/10.1002/adma.201402064.
[165] W. Seung, M.K. Gupta, K.Y. Lee, K.-S. Shin, J.-H. Lee, T.Y. Kim, et al., Nanopatterned textile-based wearable triboelectric nanogenerator, ACs Nano 9 (2015) 3501–3509, https://doi.org/10.1021/nn507221f.
[166] K.Y. Lee, H.-J. Yoon, T. Jiang, X. Wen, W. Seung, S.-W. Kim, et al., Fully packaged self-powered triboelectric pressure sensor using hemispheres-array, Adv. Energy Mater. 6 (2016) 1502566, https://doi.org/10.1002/aenm.201502566.
[167] C. Zhang, S. Liu, X. Huang, W. Guo, Y. Li, H. Wu, A stretchable dual-mode sensor array for multifunctional robotic electronic skin, Nano Energy 62 (2019) 164–170, https://doi.org/10.1016/j.nanoen.2019.05.046.
[168] Y. Wang, Z. Hu, J. Wang, X. Liu, Q. Shi, Y. Wang, et al., Deep learning-assisted triboelectric smart mats for personnel comprehensive monitoring toward maritime safety, Acs Appl. Mater. Interfaces (2022))24932–24839, https://doi.org/10.1021/acsami.2c05734.
[169] F. Gao, X. Zhao, Z. Zhang, L. An, L. Xu, X. Xun, et al., A stretching-insensitive, self-powered and wearable pressure sensor, Nano Energy 91 (2022), 106695, https://doi.org/10.1016/j.nanoen.2021.106695.
[170] T. Bu, T. Xiao, Z. Yang, G. Liu, X. Fu, J. Nie, et al., Stretchable triboelectric-photonic smart skin for tactile and gesture sensing, Adv. Mater. 30 (2018) 1800066, https://doi.org/10.1002/adma.201800066.
[171] Y.-C. Lai, J. Deng, S.L. Zhang, S. Niu, H. Guo, Z.L. Wang, Single-thread-based wearable and highly stretchable triboelectric nanogenerators and their applications in cloth-based self-powered human-interactive and biomedical sensing, Adv. Funct. Mater. 27 (2017) 1604462, https://doi.org/10.1002/adfm.201604462.
[172] Z. Zhao, Q. Huang, C. Yan, Y. Liu, X. Zeng, X. Wei, et al., Machine-washable and breathable pressure sensors based on triboelectric nanogenerators enabled by textile technologies, Nano Energy 70 (2020), 104528, https://doi.org/10.1016/j.nanoen.2020.104528.
[173] X. Zheng, W. Nie, Q. Hu, X. Wang, Z. Wang, L. Zou, et al., Multifunctional RGO/Ti3C2Tx MXene fabrics for electrochemical energy storage, electromagnetic interference shielding, electrothermal and human motion detection, Mater. Des. 200 (2021), 109442, https://doi.org/10.1016/j.matdes.2020.109442.
[174] S. Pyo, M.-O. Kim, D.-S. Kwon, W. Kim, J.-H. Yang, H.S. Cho, et al., All-textile wearable triboelectric nanogenerator using pile-embroidered fibers for enhancing output power, Smart Mater. Struct. 29 (2020), 055026, https://doi.org/10.1088/1361-665X/ab710a.
[175] X. Guan, B. Xu, M. Wu, T. Jing, Y. Yang, Y. Gao, Breathable, washable and wearable woven-structured triboelectric nanogenerators utilizing electrospun nanofibers for biomechanical energy harvesting and self-powered sensing, Nano Energy 80 (2021), 105549, https://doi.org/10.1016/j.nanoen.2020.105549.
[176] Z. Bai, Y. Xu, J. Li, J. Zhu, C. Gao, Y. Zhang, et al., An eco-friendly porous nanocomposite fabric-based triboelectric nanogenerator for efficient energy harvesting and motion sensing, ACS Appl. Mater. Interfaces 12 (2020) 42880–42890, https://doi.org/10.1021/acsami.0c12709.
[177] K. Cheng, S. Wallaert, H. Ardebili, A. Karim, Advanced triboelectric nanogenerators based on low-dimension carbon materials, A Rev., Carbon 194 (2022) 81–103, https://doi.org/10.1016/j.carbon.2022.03.037.
[178] M.-Y. Liu, C.-Z. Hang, X.-F. Zhao, L.-Y. Zhu, R.-G. Ma, J.-C. Wang, et al., Advance on flexible pressure sensors based on metal and carbonaceous nanomaterial, Nano Energy 87 (2021), 106181, https://doi.org/10.1016/j.nanoen.2021.106181.

[179] M.A. Gabris, J. Ping, Carbon nanomaterial-based nanogenerators for harvesting energy from environment, Nano Energy 90 (2021), 106494, https://doi.org/10.1016/j.nanoen.2021.106494.
[180] Y. Fang, Y. Zou, J. Xu, G. Chen, Y. Zhou, W. Deng, et al., Ambulatory cardiovascular monitoring via a machine-learning-assisted textile triboelectric sensor, Adv. Mater. 33 (2021) 2104179, https://doi.org/10.1002/adma.202104178.
[181] A. Ahmed, S.L. Zhang, I. Hassan, Z. Saadatnia, Y. Zi, J. Zu, et al., A washable, stretchable, and self-powered human-machine interfacing Triboelectric nanogenerator for wireless communications and soft robotics pressure sensor arrays, Extrem. Mech. Lett. 13 (2017) 25–35, https://doi.org/10.1016/j.eml.2017.01.006.
[182] S. Chen, T. Huang, H. Zuo, S. Qian, Y. Guo, L. Sun, et al., A single integrated 3D-printing process customizes elastic and sustainable triboelectric nanogenerators for wearable electronics, Adv. Funct. Mater. 28 (2018) 1805108, https://doi.org/10.1002/adfm.201805108.
[183] W. Yang, R. Cao, X. Zhang, H. Li, C. Li, Air-permeable and washable paper-based triboelectric nanogenerator based on highly flexible and robust paper electrodes, Adv. Mater. Technol. 3 (2018) 1800178, https://doi.org/10.1002/admt.201800178.
[184] Y. Lee, J. Kim, B. Jang, S. Kim, B.K. Sharma, J.-H. Kim, et al., Graphene-based stretchable/wearable self-powered touch sensor, Nano Energy 62 (2019) 259–267, https://doi.org/10.1016/j.nanoen.2019.05.039.
[185] H. Chu, H. Jang, Y. Lee, Y. Chae, J.-H. Ahn, Conformal, graphene-based triboelectric nanogenerator for self-powered wearable electronics, Nano Energy 27 (2016) 298–305, https://doi.org/10.1016/j.nanoen.2016.07.009.
[186] J. Yang, P. Liu, X. Wei, W. Luo, J. Yang, H. Jiang, et al., Surface engineering of graphene composite transparent electrodes for high-performance flexible triboelectric nanogenerators and self-powered sensors, ACS Appl. Mater. Interfaces 9 (2017) 36017–36025, https://doi.org/10.1021/acsami.7b10373.
[187] H. Guo, T. Li, X. Cao, J. Xiong, Y. Jie, M. Willander, et al., Self-sterilized flexible single-electrode triboelectric nanogenerator for energy harvesting and dynamic force sensing, ACS Nano 11 (2017) 856–864, https://doi.org/10.1021/acsnano.6b07389.
[188] L. Huang, J. Su, Y. Song, R. Ye, Laser-induced graphene: en route to smart sensing, Nano-Micro Lett. 12 (2020), https://doi.org/10.1007/s40820-020-00496-0.
[189] T. Han, A. Nag, N. Afsarimanesh, S.C. Mukhopadhyay, S. Kundu, Y. Xu, Laser-assisted printed flexible sensors, A Rev., Sens. 19 (2019), https://doi.org/10.3390/s19061462.
[190] H. Wang, Z. Xiang, J. Wan, Y. Song, H. Zhang, Ieee, DOUBLE-SIDED LASER-INDUCED GRAPHENE BASED SMART BRACELET FOR SENSING AND ENERGY, 34th IEEE International Conference on Micro Electro Mechanical Systems (MEMS), (2021) 34–37.https://doi.org/10.1109/mems51782.2021.9375415.
[191] L.-Q. Tao, H. Tian, Y. Liu, Z.-Y. Ju, Y. Pang, Y.-Q. Chen, et al., An intelligent artificial throat with sound-sensing ability based on laser induced graphene, Nat. Commun. 8 (2017) 14579, https://doi.org/10.1038/ncomms14579.
[192] K. Zhou, Y. Zhao, X. Sun, Z. Yuan, G. Zheng, K. Dai, et al., Ultra-stretchable triboelectric nanogenerator as high-sensitive and self-powered electronic skins for energy harvesting and tactile sensing, Nano Energy 70 (2020), 104546, https://doi.org/10.1016/j.nanoen.2020.104546.
[193] L. Yang, C. Liu, W. Yuan, C. Meng, A. Dutta, X. Chen, et al., Fully stretchable, porous MXene-graphene foam nanocomposites for energy harvesting and self-powered sensing, Nano Energy 103 (2022), 107807, https://doi.org/10.1016/j.nanoen.2022.107807.
[194] Y. Li, W. Zheng, H. Zhang, H. Wang, H. Cai, Y. Zhang, et al., Electron transfer mechanism of graphene/Cu heterostructure for improving the stability of triboelectric nanogenerators, Nano Energy 70 (2020), 104540, https://doi.org/10.1016/j.nanoen.2020.104540.
[195] H. Chen, W. Yang, P. Huang, C. Li, Y. Yang, B. Zheng, et al., A multiple laser-induced hybrid electrode for flexible triboelectric nanogenerators, Sustain. Energy Fuels 5 (2021) 3737–3743, https://doi.org/10.1039/d1se00819f.
[196] X. Zhao, D. Zhang, S. Xu, W. Qian, W. Han, Z.L. Wang, et al., Stretching-enhanced triboelectric nanogenerator for efficient wind energy scavenging and ultrasensitive strain sensing, Nano Energy 75 (2020), 104920, https://doi.org/10.1016/j.nanoen.2020.104920.
[197] Y. Long, Z. Wang, F. Xu, B. Jiang, J. Xiao, J. Yang, et al., Mechanically ultra-robust, elastic, conductive, and multifunctional hybrid hydrogel for a triboelectric nanogenerator and flexible/wearable sensor, Small (2022))2203956, https://doi.org/10.1002/smll.202203956.
[198] F. He, X. You, H. Gong, Y. Yang, T. Bai, W. Wang, et al., Stretchable, biocompatible, and multifunctional silk fibroin-based hydrogels toward wearable strain/pressure sensors and triboelectric nanogenerators, ACS Appl. Mater. Interfaces 12 (2020) 6442–6450, https://doi.org/10.1021/acsami.9b19721.

Linan Guo is currently pursuing the master's degree in Dalian Maritime University, China. His current research work focuses on Triboelectric Nanogenerator and the bionic whisker sensor based on the triboelectric nanogenerators.

Guitao Wu graduated from Dalian Maritime University with a doctor's degree in marine engineering in 2005. He has been a professor in Dalian Maritime University since 2007, mainly engaged in the research work of modern marine engineering management. His research focuses on intelligent ships, green ships as well as energy capture and self-driving sensing based on triboelectric nanogenerators.

Qunyi Wang is currently pursuing the master's degree in Dalian Maritime University, China. His current research direction is the self-powered system of vibration measurement and triboelectric nanogenerators.

Tong Li, currently studying for MASTER's degree at Dalian Maritime University. Her current research interest is in microfluidic systems for ocean salinity gradient power generation.

Bohan Yao is currently pursuing the master's degree in Dalian Maritime University, China. His current research direction is the self-powered system of vibration measurement and triboelectric nanogenerators.

Yongjiu Zou is an assistant professor at College of Marine Engineering, Dalian Maritime University. He received his B.S. and M.S. in marine engineering both from Dalian Maritime University in 2012 and 2014, respectively. His research focuses on triboelectric nanogenerators for energy harvesting and self-powered sensors.

Minyi Xu received his Ph.D. degree from Peking University in 2012. During 2016–2017, he joined Professor Zhong Lin Wang' group at Georgia Institute of Technology. Now he is a Professor in the Marine Engineering College, Dalian Maritime University. His current research is mainly focused on the areas of blue energy, self-powered systems, triboelectric nanogenerators and its practical applications in smart ship and ocean.